

**Final report for iBSc/MEng Project**

---

**Construction and Characterisation of a library of toggle switches in *Escherichia coli***

---

**Author name(s):**

**Adnan Gondal, Sam Karet, Hyung Jip Lee, Jaeyun Lee, Clinton Ng, Qingwei Zhang**

Supervisor(s): Professor Kitney, Dr Matthieu Bultelle, Dr Charles Motraghi and Mr Alexis Casas

Submitted in partial fulfilment of the requirements for the award of BEng/MEng in Biomedical Engineering from Imperial College London

March 2020

Word count: 4891

Feedback box for project markers:

WHAT could/should be improved:

## Table of Contents

<b>1. ABSTRACT</b>	<b>3</b>
<b>2. ACKNOWLEDGEMENTS</b>	<b>3</b>
<b>3. INTRODUCTION</b>	<b>5</b>
3.1 AIMS	5
3.2 BACKGROUND	5
3.2.1 SYNTHETIC BIOLOGY	5
3.2.2 TOGGLE SWITCH	7
3.2.3 APPLICATIONS	7
<b>4. MODELLING</b>	<b>8</b>
4.1 TOGGLE SWITCH MODEL DERIVATION	8
4.2 DRYLAB MODEL ANALYSIS	12
4.2.1 PLOTTING OF NULLCLINES AND FIXED POINTS	12
4.2.2 IMPORTANCE OF COOPERATIVITY	13
4.2.3 PARAMETER SENSITIVITY OF BISTABILITY	14
4.2.4 FLOW DIAGRAMS	15
<b>5. EXPERIMENTAL STRATEGY (WET LAB)</b>	<b>18</b>
5.1 OVERVIEW OF TECHNIQUES	18
5.2 <i>IN SILICO</i> ASSEMBLY (BENCHLING)	21
5.3 METHODS AND PROTOCOLS ( <i>IN VITRO</i> ASSEMBLY)	29
<b>6. EXPERIMENTAL RESULTS</b>	<b>31</b>
<b>7. DISCUSSION</b>	<b>36</b>
<b>8. WIKI</b>	<b>37</b>
<b>9. FUTURE WORK</b>	<b>38</b>
<b>10. REFERENCES</b>	<b>39</b>
<b>APPENDICES</b>	<b>41</b>
APPENDIX A – PROJECT ORGANISATION	41
APPENDIX B – JACOBIAN MATRIX FOR TOGGLE SWITCH SYSTEM	41
APPENDIX C – <i>IN SILICO</i> PRIMER SEQUENCES AND DESIGN GUIDELINES	42
APPENDIX D – LIST OF PARTS ORDERED FROM ADDGENE/THERMOFISHER	43
APPENDIX E – PROTOCOLS	43
APPENDIX F – PRIMER SEQUENCE AND GUIDELINES FOR ALIGNMENT AND ANALYSIS	47
APPENDIX G – LIST OF PLATE READER EXPERIMENTS	47
APPENDIX H – SUMMARY OF RESULTS (ALL TESTED TOGGLE SWITCHES)	48

## 1. Abstract

Synthetic biology is a multidisciplinary field that involves the integration of knowledge from biology and chemistry; with the aim of designing and engineering new biologically based parts, devices and systems, as well as the redesign of existing natural biological systems.<sup>[4]</sup> The purpose of this project was to understand the synthetic biology design process by implementing the design, analysis and construction of a simple system. An initial literature review was undertaken on synthetic biology systems and applications, and it was decided that the system this project will focus on will be the toggle switch design by Gardner et al.<sup>[1]</sup> This system consists of two repressors and two constitutive promoters, and each promoter is inhibited by the repressor that is transcribed by the opposing promoter.

A mathematical model of the toggle switch was derived from first principles. This model was subsequently analysed to identify parameters that give rise to a Toggle Switch with Bistability, by analysis of the steady state behaviour of the system with the help of simulations via Python.

Toggle switch constructs were created and assembled *in silico* using Benchling. Several constituent parts were successfully minipreped, cultured and transformed in *E. coli* DH5 $\alpha$  - these plasmids were sent for alignment analysis to confirm the sequence. Pre-constructed toggle switches from Addgene (based on Collin's design) were ordered and tested for chassis compatibility in  $\Delta$ lacI/ $\Delta$ araC *E. coli*. The fluorescence and optical density were recorded using a plate reader. 3 toggle switches in 2 chassis were successful to varying degrees. Furthermore, preliminary work on assembling modular components for a *de novo* toggle switch were successful.

## 2. Acknowledgements

Special thanks to Professor Richard Kitney for his continued support and guidance throughout the project. We would also like to thank Dr Matthieu Bultelle, Dr Charles Motraghi, and Mr Alexis Casas, for all their guidance and support with the planning, wetlab, and drylab portions of the project.

Additional thanks to Ms Tania Briggs for her role in organising weekly meetings.

**Abbreviations used in this report:**

CIDAR: Cross-disciplinary Integration of Design Automation Research

DNA: deoxyribonucleic acid

GFP: green fluorescent protein

GPP: geranyl pyrophosphate

iGEM: International Genetically Engineered Machine

IPTG: Isopropyl  $\beta$ -D-1-thiogalactopyranoside

MoClo: Modular Cloning

mRNA: messenger ribonucleic acid

ODEs: ordinary differential equations

PCR: polymerase chain reaction

pDVA: Plasmid DNA Vector Ampicillin

pDVK: Plasmid DNA Vector Kanamycin

RBS: Ribosome Binding sites

ATc: anhydrotetracycline

*E. coli*: *Escherichia coli*

### 3. Introduction

#### 3.1 Aims

The general aim of this project is to experience the synthetic biology process - the use of engineering principles to design and build a biologically based system. Our project involves the construction and characterization of the genetic toggle switch<sup>[1]</sup> - a well-known biological construct. The project has two main components:

- The implementation of computational analysis of a toggle switch model.
- The wetlab construction and testing of the toggle switch.

The objectives of this project are as follows:

- To construct and characterise a working toggle switch *de novo*.
- To test a pre-constructed toggle switch *in vitro* in *E. coli*  $\Delta$ lacI/ $\Delta$ araC and BL21 to test chassis compatibility

The objective of this report is to outline both the progress made with the project and our theoretical understanding of the subject.

#### 3.2 Background

##### 3.2.1 Synthetic Biology

Synthetic biology is the application of engineering principles to biology.<sup>[2]</sup> This multidisciplinary field involves the integration of knowledge from biology, engineering and chemistry (*Figure 1*); with aims to design and construct novel parts or redesign existing biological systems. Subsequently, these can be characterised and modelled, and documented for universal use.<sup>[3]</sup>

The building blocks of a synthetic biology system, i.e. its constituent parts, should be designed with modularity and orthogonality in mind. Modular parts have discrete functions and hence can be arranged and combined to build more complex and customisable systems. Orthogonal parts do not interact ('cross-talk') with each other, or constituent host processes. Unlike other engineering disciplines, programming living organisms lack predictability, due to unknown or unforeseen biochemical interactions. Consequently, *in silico* designs must undergo extensive *in vitro* testing to ensure prediction match the results— the results of which can be used to complete iteration of the design cycle.<sup>[3]</sup>

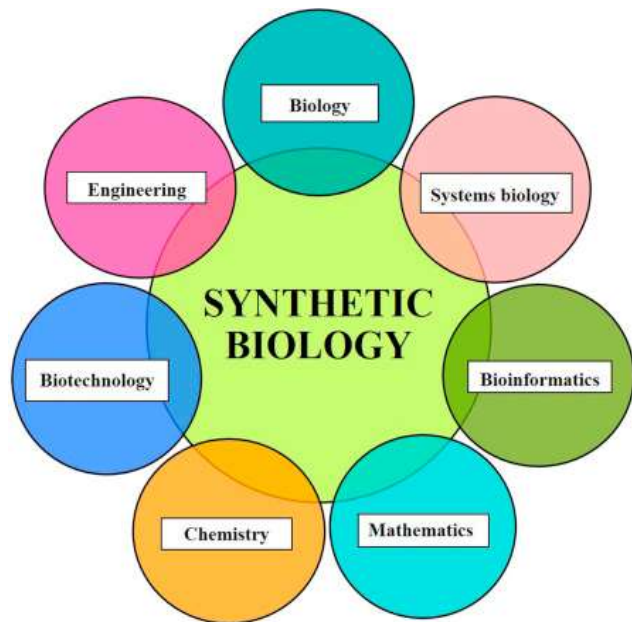


*Figure 1.* Synthetic Biology comprises multiple disciplines <sup>[4]</sup>

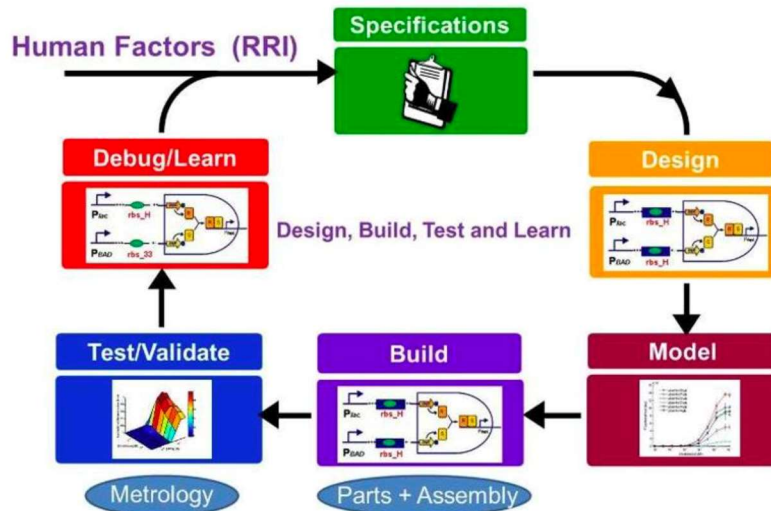


Figure 2. The Design Cycle for Synthetic Biology <sup>[3]</sup>

There is a large range of applications that synthetic biology will have an impact on in the future. It can solve problems in a wide range of sectors including healthcare, energy and agriculture, and tackle challenges for which the current technology is insufficient whilst using renewable and potentially low-carbon biological materials.<sup>[5]</sup> Biological circuits can be placed into host cells to exploit the sustainable cell and DNA replication potential.

Chassis are cells into which engineered genetic circuits are implanted into;<sup>[3]</sup> they provide metabolic resources and machinery that support its functioning. *Escherichia coli* are commonly used for similar projects, owing to several reasons:

- Fast growth rate and inexpensive substrate requirements
- Extensive knowledge of its metabolism and genetic material
- Non-toxicity in human applications (most laboratory strains rated biosafety level 1).<sup>[6]</sup>

Successful toggle switches have been assembled in *E. coli*.<sup>[1, 7-9]</sup>

### 3.2.2 Toggle Switch

A toggle switch is a ‘bistable gene-regulatory network’, which allows switching between two distinct steady states.<sup>[1]</sup> A literature review<sup>[10-15]</sup> suggests that numerous works are based on Gardner et al’s fundamental design of the first robust biological toggle switch (*Figure 3*).<sup>[1]</sup>

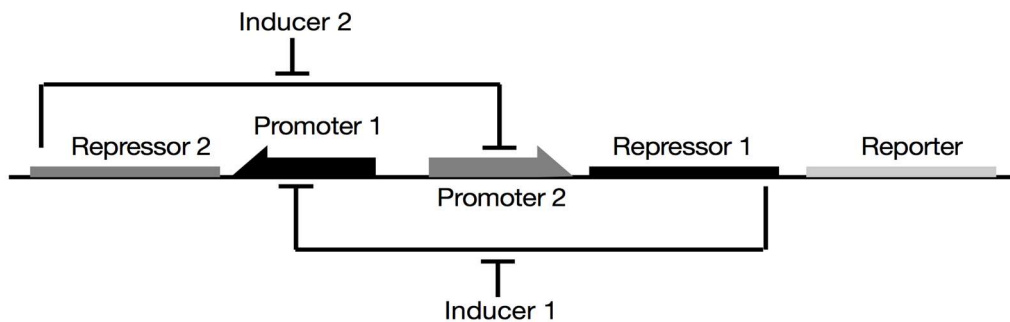


*Figure 3.* Structure of Gardner’s genetic toggle switch<sup>[1]</sup>

This design consists of two promoters and their constitutive genes arranged in a mutually inhibitory configuration – each promoter is inhibited by repressor protein produced by the opposing promoter’s gene. The transient presence of an inducer permits the maximal transcription of one repressor, which alters the dynamic balance between competing promoters and enables switching into one state. Conversely, switching into the other state is triggered by introducing an inducer of the opposing repressor.

### 3.2.3 Applications

A plethora of toggle switch applications exist, mainly in genetic therapy, metabolic engineering, and pharmaceutical development.<sup>[16, 17]</sup> By coupling inducers to signal recognition molecules and placing the toggle switch upstream of a protein sequence in a host chassis (e.g. *E. coli.*), biosensors can be fabricated and consequently used in gene regulation.<sup>[18]</sup> Medical applications include: switches controlled by antibiotics, immunosuppressive drugs, and hormones, and biosensors controlled by physical factors e.g. temperature, electricity and light.<sup>[19-24]</sup>

## 4. Modelling

### 4.1 Toggle Switch Model Derivation

Gardner's toggle switch is composed of two repressors and two constitutive promoters. Each promoter is inhibited by the repressor that is transcribed by the opposing promoter. [1] A mathematical model of the toggle switch has been derived from first principles and this is as follows.

#### Chemical reactions of toggle switch

Protein A	Protein B
Transcription: $\text{DNA} \xrightarrow{K_{1,A} * g(p_B)} \text{DNA} + \text{mRNA}_A$	Transcription: $\text{DNA} \xrightarrow{K_{1,B} * f(p_A)} \text{DNA} + \text{mRNA}_B$
Translation: $\text{mRNA}_A \xrightarrow{K_{2,A}} \text{mRNA}_A + \text{protein}_A$	Translation: $\text{mRNA}_B \xrightarrow{K_{2,B}} \text{mRNA}_B + \text{protein}_B$
Degradation of mRNA: $\text{mRNA}_A \xrightarrow{d_{1,A}} \emptyset$	Degradation of mRNA: $\text{mRNA}_B \xrightarrow{d_{1,B}} \emptyset$
Degradation of protein: $\text{protein}_A \xrightarrow{d_{2,A}} \emptyset$	Degradation of protein: $\text{protein}_B \xrightarrow{d_{2,B}} \emptyset$

*Table 1: Chemical equations of gene expression*

The following points describe the notations used:

1. The transcription rate is attenuated by following Hill equations:

$$f(p_A) = \frac{K_{M,A}^\gamma}{K_{M,A}^\gamma + p_A^\gamma}, \quad g(p_B) = \frac{K_{M,B}^\beta}{K_{M,B}^\beta + p_B^\beta}$$

$K_{M,A}$  = repression coefficient for protein A

$K_{M,B}$  = repression coefficient for protein A

$\gamma$  = Cooperativity of protein A,  $\beta$  = Cooperativity of protein B

2. The translation rate parameters are given by:

$K_{2,A}$  and  $K_{2,B}$  = translation rate for protein A and protein B respectively

3. The protein and mRNA degradation rate parameters are given by:

$d_{1,A}$  and  $d_{1,B}$  are degradation rates of mRNA A and B respectively

$d_{2,A}$  and  $d_{2,B}$  are degradation rates of protein A and B respectively

## ODEs of the system

The Law of Mass Action<sup>[18]</sup> yields the ODE's below:

$$\left\{ \begin{array}{l} \frac{dm_A}{dt} = K_{1,A} \frac{K_{M,B}^\beta}{K_{M,B}^\beta + p_B^\beta} - d_{1,A}m_A \quad (1) \\ \frac{dm_B}{dt} = K_{1,B} \frac{K_A^\gamma}{K_{M,A}^\gamma + p_A^\gamma} - d_{1,B}m_B \quad (2) \\ \frac{dp_A}{dt} = K_{2,A}m_A - d_{2,A}p_A \quad (3) \\ \frac{dp_B}{dt} = K_{2,B}m_B - d_{2,B}p_B \quad (4) \end{array} \right.$$

We let  $m_A = [mRNA_A]$ ,  $m_B = [mRNA_B]$  and  $p_A = [protein_A]$ ,  $p_B = [protein_B]$

We make Quasi Stationary approximation for mRNA concentration, where we assume the concentration of mRNA is constant over time.<sup>[19]</sup> This is because it is understood that the concentrations in the system will go to steady state, and that the mRNA concentrations reach a steady state much faster (in a few minutes) compared to the protein concentrations (that take a few hours).

This makes  $\dot{m}_A = 0$  and  $\dot{m}_B = 0$ . Rearranging equations 1 and 2 yields:

$$m_A = \frac{K_{1,A}}{d_{1,A}} \frac{K_{M,B}^\beta}{K_{M,B}^\beta + p_B^\beta}$$

$$m_B = \frac{K_{1,B}}{d_{1,B}} \frac{K_A^\gamma}{K_{M,A}^\gamma + p_A^\gamma}$$

Substituting this result into equation 3 gives:

$$\frac{dp_A}{dt} = K_{2,A} \frac{K_{1,A}}{d_{1,A}} \frac{K_{M,B}^\beta}{K_{M,B}^\beta + p_B^\beta} - d_{2,A}p_A \quad (5)$$

$$\frac{dp_B}{dt} = K_{2,B} \frac{K_{1,B}}{d_{1,B}} \frac{K_A^\gamma}{K_{M,A}^\gamma + p_A^\gamma} - d_{2,B}p_B \quad (6)$$

## Normalisation

The aim is to obtain a more parsimonious model that can be described by fewer parameters. We know that the protein degradation rate is the same for both protein A and protein B because proteins are stable and that the degradation rate is made of 2 terms: the degradation rate of the species itself and the dilution rate which represents the change in volume through time. In our case, the proteins are very stable meaning that the first term is negligible, which only leaves the dilution rate. Thus, the protein degradation rate can be approximated to the dilution rate.

We also change the timescale:

$$t_s = t\alpha \rightarrow t = \frac{t_s}{\alpha}$$

Substituting this into equation 5 and 6 gives:

$$\begin{aligned} \frac{dp_A}{dt} &= \frac{dp_A}{d\left(\frac{t_s}{\alpha}\right)} = \alpha \frac{dp_A}{dt_s} = K_{2,A} \frac{K_{1,A}}{d_{1,A}} \frac{K_{M,B}^\beta}{K_{M,B}^\beta + p_B^\beta} - d_2 p_A \\ \frac{dp_B}{dt} &= \frac{dp_B}{d\left(\frac{t_s}{\alpha}\right)} = \alpha \frac{dp_B}{dt_s} = K_{2,B} \frac{K_{1,B}}{d_{1,B}} \frac{K_{M,A}^\gamma}{K_{M,A}^\gamma + p_A^\gamma} - d_2 p_B \end{aligned}$$

Rearranging and choosing the value  $\alpha = d_2$  yields:

$$\frac{dp_A}{dt_s} = \frac{K_{2,A} K_{1,A}}{d_2} \frac{K_{M,B}^\beta}{d_{1,A} K_{M,B}^\beta + p_B^\beta} - p_A \quad (7)$$

$$\frac{dp_B}{dt_s} = \frac{K_{2,B} K_{1,B}}{d_2} \frac{K_{M,A}^\gamma}{d_{1,B} K_{M,A}^\gamma + p_A^\gamma} - p_B \quad (8)$$

Using the normalized version of the Hill function:

$$\begin{aligned} f(p_A) &= \frac{K_{M,A}^\gamma}{K_{M,A}^\gamma + p_A^\gamma} = \frac{1}{1 + \left(\frac{p_A}{K_{M,A}}\right)^\gamma} \\ g(p_B) &= \frac{K_{M,B}^\beta}{K_{M,B}^\beta + p_B^\beta} = \frac{1}{1 + \left(\frac{p_B}{K_{M,B}}\right)^\beta} \end{aligned}$$

The dimensionless concentrations U and V are defined as:

$$U = \frac{p_A}{K_{M,A}} \quad \text{and} \quad V = \frac{p_B}{K_{M,B}}$$

Therefore, equation 7 can be written as:

$$\begin{aligned} \frac{dp_A}{dt_s} &= K_{M,A} \frac{dU}{dt_s} = \frac{K_{2,A} K_{1,A}}{d_{2,A} d_{1,A}} \frac{1}{1 + V^\beta} - K_{M,A} U \\ \frac{dU}{dt_s} &= \frac{K_{2,A} K_{1,A}}{K_{M,A} d_{2,A} d_{1,A}} \frac{1}{1 + V^\beta} - U \end{aligned}$$

Defining a lumped parameter  $\alpha_1 = \frac{K_{2,A}K_{1,A}}{K_{M,A}d_2d_{1,A}}$ , which is maximum steady state concentration rescaled by  $K_{M,A}$ .

Substituting it into above equation gives:

$$\frac{dU}{dt_s} = \frac{\alpha_1}{1 + V^\beta} - U$$

Similar analysis for equation (8) and defining  $\alpha_2 = \frac{K_{2,B}K_{1,B}}{K_{M,B}d_2d_{1,B}}$ , which is maximum steady state concentration rescaled by  $K_{M,B}$ .

$$\frac{dV}{dt_s} = \frac{\alpha_2}{1 + U^\gamma} - V$$

Finally, yielding the same system as Gardner et Al:

$$\begin{cases} \frac{dU}{dt_s} = \frac{\alpha_1}{1 + V^\beta} - U \\ \frac{dV}{dt_s} = \frac{\alpha_2}{1 + U^\gamma} - V \end{cases}$$

Where U, V are the normalised concentrations of the repressors,  $\alpha_1$  and  $\alpha_2$  are the maximum rate of U and V synthesis respectively and  $\beta$  and  $\gamma$  are the cooperativities of the repressors.

## 4.2 Drylab Model Analysis

The motivation for the analysis below is to have an understanding of the conditions that can give a working genetic toggle switch, and therefore we look for the steady states of the system. Bistability of the system is not always achieved and depends on the parameters.

All simulations have been done via Jupyter notebook and the code has been uploaded to google colab and can be found at:

[https://colab.research.google.com/drive/103AxiByb8octTdOuE\\_8aY4yKioacK3Hu](https://colab.research.google.com/drive/103AxiByb8octTdOuE_8aY4yKioacK3Hu)

### 4.2.1 Plotting of Nullclines and Fixed Points.

The steady states of the system correspond to the solutions of  $\frac{dU}{dt_s} = \frac{dV}{dt_s} = 0$  :

$$\begin{cases} U = \frac{\alpha_1}{1 + V^\beta} \\ V = \frac{\alpha_2}{1 + U^\gamma} \end{cases}$$

As it is not possible to solve the above equations analytically, we undertake nullcline analysis of the model. Here each of the derivatives with respect to time is set equal to zero and the corresponding lines are plotted.

The plot of the nullclines and the numerical solutions for one set of parameters are shown in *Figure 4*. The steady states correspond to the intersections of the nullclines.

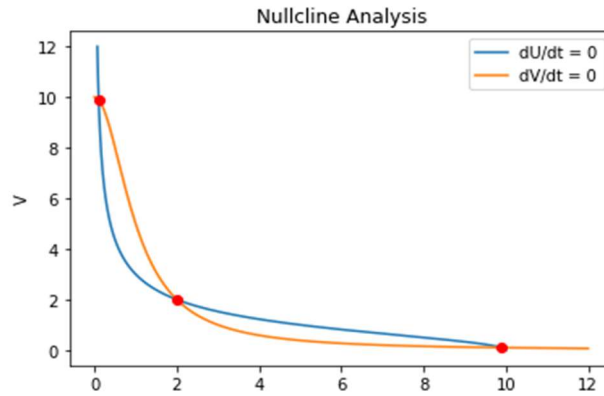


*Figure 4.* Parameters:  $\alpha_1 = 10$ ,  $\alpha_2 = 10$ ,  $\beta = 2$  and  $\gamma = 2$

To study the local stability of the system, eigenvalues of the Jacobian matrices at each of the fixed points was computed. (*Appendix B*)

The eigenvalues of each of the fixed points are presented in *Table 2*:

Steady Point	Eigenvalue 1	Eigenvalue 2
(0.101,9.899)	-0.800	-1.199
(9.899,0.101)	-0.800	-1.199
(2.0,2.0)	0.600	-2.600

*Table 2.* Steady points and eigenvalues

The real parts of the eigenvalues of the steady points at  $[0.1, 9.8]$  and at  $[9.8, 0.1]$  are negative which indicates that these points are stable attractive nodes. For the fixed point at  $([2,2])$  the real part of one of the eigenvalues is positive and for the other it is negative. This means that it is stable in one direction but unstable in the other- a Saddle Point. It can thus be concluded that the above parameters give two stable steady states and the corresponding system is a toggle switch.

The plot of the Nullclines and numerical solutions for a different set of parameters, that do not give a toggle switch as there is only one steady point, are shown in *Figure 5*.

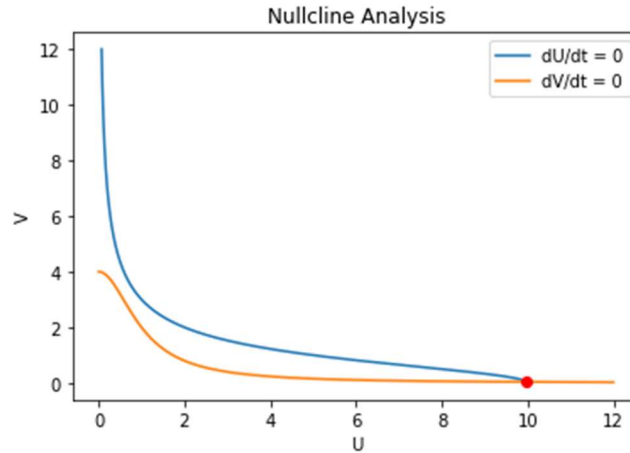


*Figure 5.* Parameters:  $\alpha_1 = 10$  ,  $\alpha_2 = 4$ ,  $\beta = 2$  and  $\gamma = 2$

#### 4.2.2 Importance of Cooperativity

The parameters  $\beta$  and  $\gamma$  represent the cooperativities of the promoters of the respective repressors. When these parameters are equal to 1 (no cooperativity in the promoters), the model becomes:

$$\begin{cases} \frac{dU}{dt} = \frac{\alpha_1}{1+V} - U \\ \frac{dV}{dt} = \frac{\alpha_2}{1+U} - V \end{cases}$$

At steady state:

$$U = \frac{\alpha_1}{1+V} \quad (1)$$

$$V = \frac{\alpha_2}{1+U} \quad (2)$$

Which can be rearranged to give the quadratic expression:

$$U^2 + U(\alpha_2 - \alpha_1 + 1) - \alpha_1 = 0$$

From inspection we know that the equation above will only have one acceptable (positive) solution, thus Bistability can never be achieved.

### 4.2.3 Parameter Sensitivity of Bistability

Looking at the parameters constituted in the lumped Parameters  $a_1$  and  $a_2$ :

$$\alpha_1 = \frac{K_{2,A}K_{1,A}}{K_{M,A}d_2d_{1,A}} \quad \alpha_2 = \frac{K_{2,B}K_{1,B}}{K_{M,B}d_2d_{1,B}}$$

- $K_1$  depends on the promoter, which is difficult to modify because promoter engineering is very complicated and there is no forward model to predict it.
- $K_2$  depends on the Ribosome Binding Site (RBS), which is a short sequence in the mRNA that can be tuned, and behaviour can be predicted via RBS calculators.
- $d_1$  is the mRNA degradation rate which cannot be modified easily or rationally.
- $d_2$  is the protein degradation rate which depends on the dilution rate and cannot be modified.

As well as this,  $\beta$  and  $\gamma$  are cooperativities that depend on the promoter, and are usually obtained experimentally. Therefore, it is sensible to modify  $a_1$  and  $a_2$  as they can also be modified practically, via RBS engineering with fixed Promoters. The Bifurcation diagrams in *Figure 6* illustrate how changing  $a_1$  and  $a_2$  impacts the system for given values of the hill coefficient.

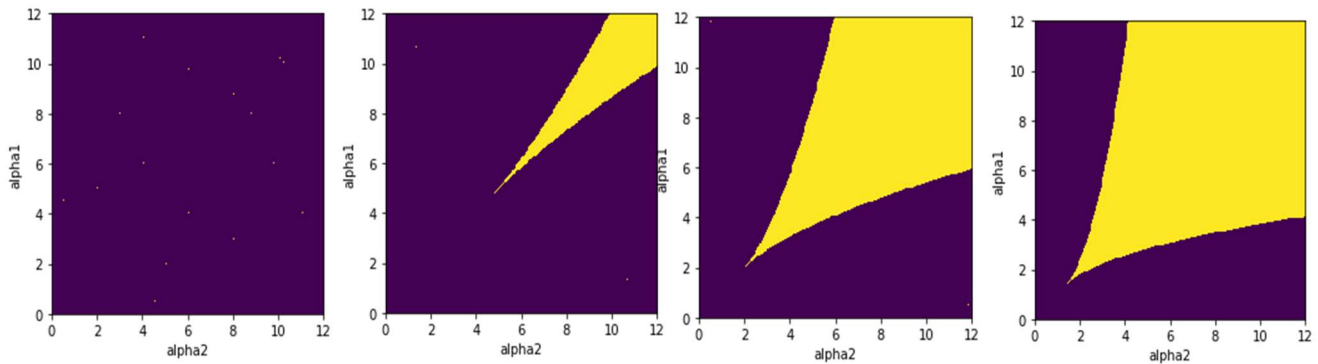


**Figure 6.** (a)  $\beta = 1, \gamma = 1$

(b)  $\beta = 1.5, \gamma = 1.5$

(c)  $\beta = 2, \gamma = 2.$

(d)  $\beta = 2.5, \gamma = 2.5$

In *Figure 6*, the yellow area represents the set of parameters that gives rise to bistability which defines a toggle switch, whereas the purple area represents the set of parameters that do not define a toggle switch.

Some conclusions we can make from these plots are:

- *Figure 6* (a) shows that no cooperativity in the promoters does not define a Toggle Switch.
- Higher cooperativity gives a larger range of  $\alpha_1$  and  $\alpha_2$  values that define a toggle switch. This can be observed in (b) (c) and (d) that the yellow region that defines the toggle switch increases as the cooperativities of each of the promoters increase.

#### 4.2.4 Flow Diagrams

For the toggle switch the steady state that the system reaches, and how quickly it does this, depends on the initial conditions (initial concentrations of repressors). To further understand the behaviour around the steady points, different plots can be computed that describe the flow of the system.

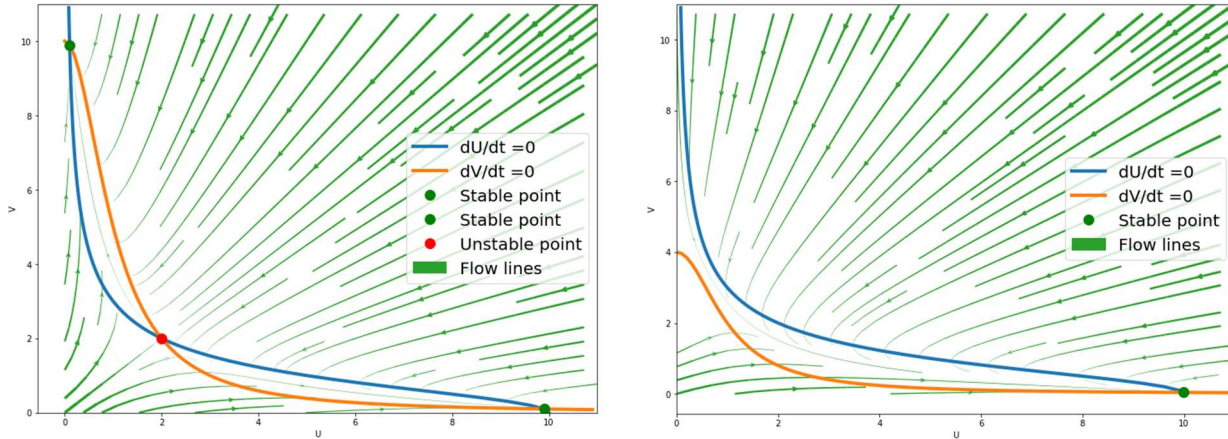


**Figure 7.** Flow diagram with direction. Left: toggle switch case ( $a_1 = 10$ ,  $\alpha_2 = 10$ ,  $\beta = 2$  and  $\gamma = 2$ )  
Right: non-toggle switch case ( $a_1 = 10$ ,  $\alpha_2 = 4$ ,  $\beta = 2$  and  $\gamma = 2$ )

*Figure 7* shows, as well as the nullclines and the fixed points, the flow lines for the system. (a) is the dynamic flow of when the parameters yield a bistable system with two stable steady points, which are represented by green dots. Flow of the system is symmetrical due to the symmetry in parameters. The streamlines can be used to identify the basin of attraction of each of the steady points. (b) Dynamic flow of system with parameters that yield a monostable system which does not define a Toggle Switch.

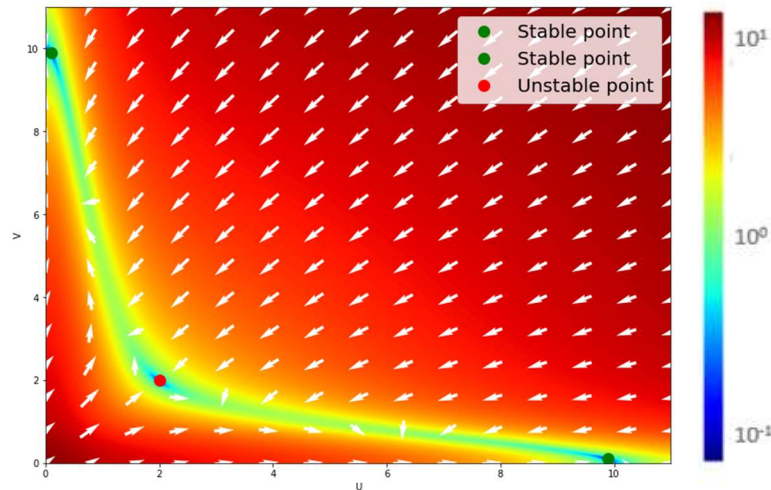


**Figure 8.** Flow diagram with magnitude and direction. Parameter values are  $a_1 = 10$ ,  $\alpha_2 = 10$ ,  $\beta = 2$  and  $\gamma = 2$

*Figure 8* adds the flow magnitude to as well as the flow so it illustrates the vector fields for different initial concentrations of  $U$  and  $V$ . A red colour means that the system returns to steady state faster whilst blue is smaller magnitudes of flow. When concentrations are far from steady state, the system returns faster to a possible steady state. Conversely when concentrations are closer to a steady state, the system takes longer to return to the steady state.

## Influence of $a_1$ and $\alpha_2$

Effect of changing  $a_1$  and  $\alpha_2$  are shown in the flow diagrams below.

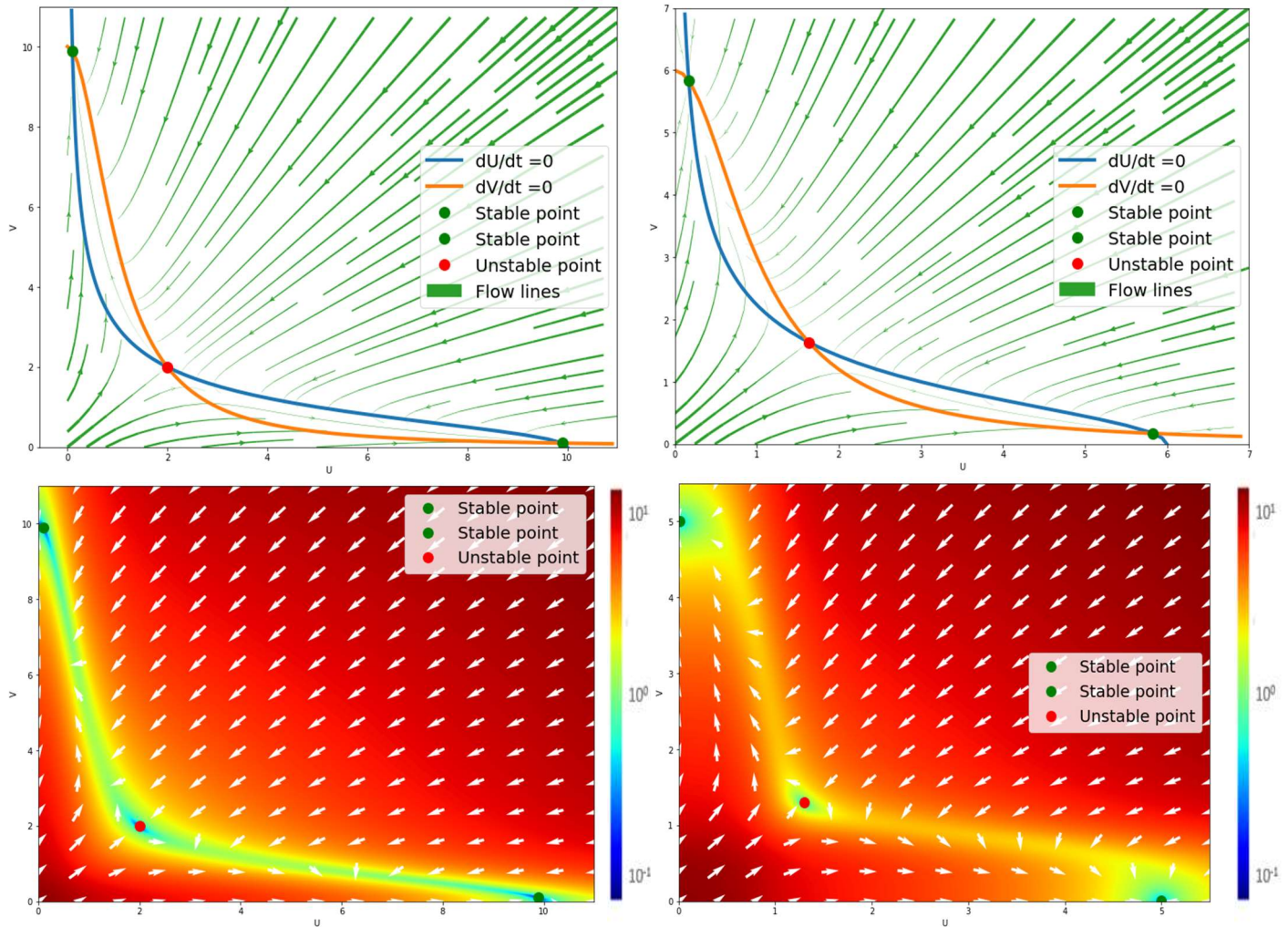


**Figure 9.** Parameter sensitivity simulation results. Left (a) Parameters:  $a_1 = 10$ ,  $\alpha_2 = 10$ ,  $\beta = 2$  and  $\gamma = 2$ .

Right (b) Parameters:  $a_1 = 6$ ,  $\alpha_2 = 6$ ,  $\beta = 2$  and  $\gamma = 2$ .

*Figure 9* describes how different parameters impact the flow and flow magnitude. The results are shown for equal values of  $a_1$  and  $\alpha_2$ , and it is observed that higher values of  $a_1$  and  $\alpha_2$  causes increased flow magnitude and the separation of steady states, which means the system returns to the steady points faster and the steady states are further apart.

## Influence of Hill Coefficient

The effect of changing the Hill Coefficients  $\beta$  and  $\gamma$  on the flow are shown below.

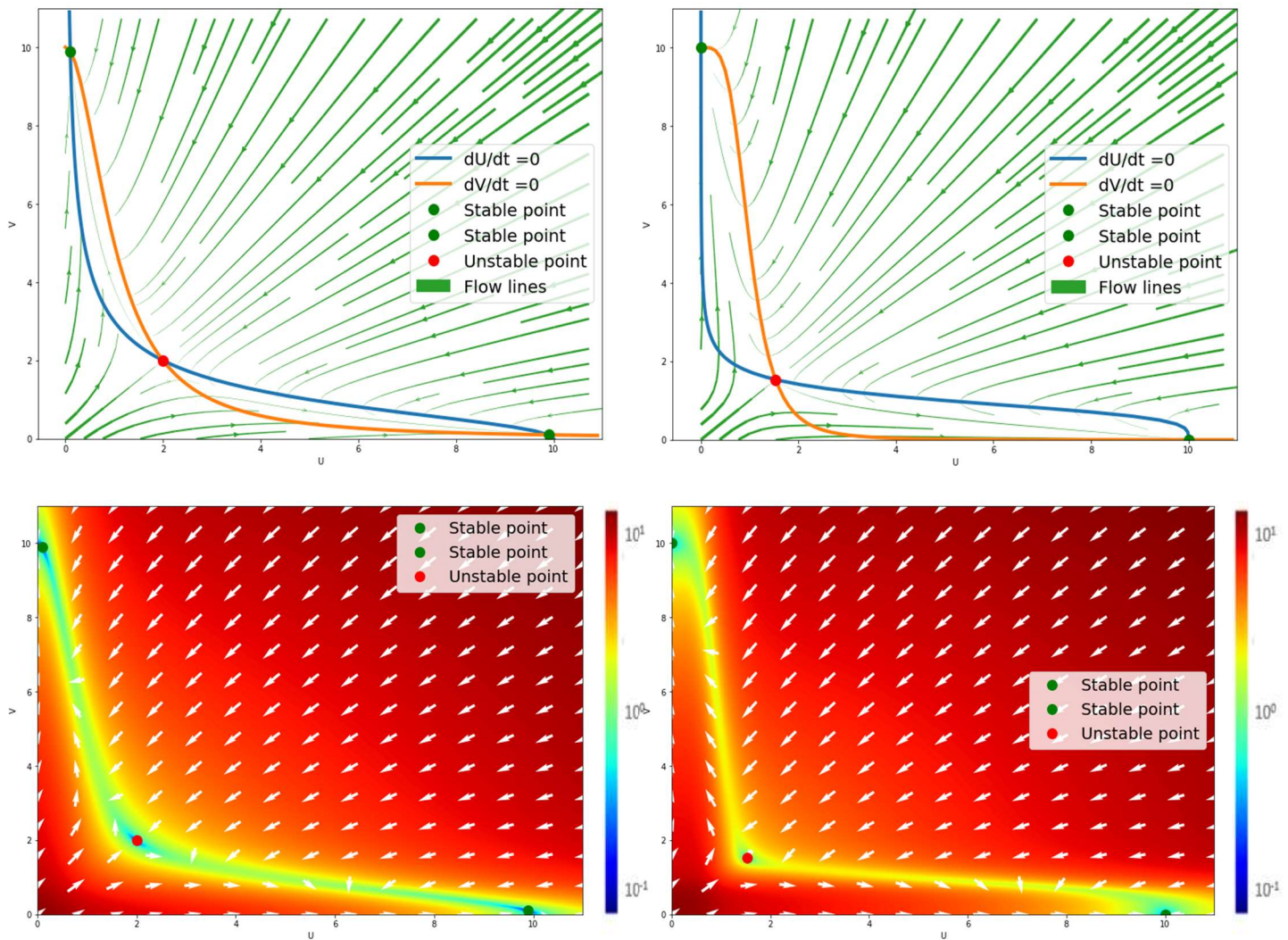


**Figure 10.** Simulation results for influence of Hill coefficient.

Left (a) Parameters:  $a_1 = 10$ ,  $\alpha_2 = 10$ ,  $\beta = 2$  and  $\gamma = 2$ .

Right (b) Parameters:  $a_1 = 10$ ,  $\alpha_2 = 10$ ,  $\beta = 4$  and  $\gamma = 4$ .

From *Figure 10*, it is observed that increasing Hill coefficients results in an increase in the separation between the Nullclines which gives a larger magnitude of flow meaning that the time taken to reach steady state increases. The blue and green areas corresponding to a slow return to the steady state also become smaller, especially at the vicinity of the unstable point.

## 5. Experimental Strategy (Wet Lab)

### 5.1 Overview of Techniques

A combination of Golden Gate Assembly and Gibson's Assembly techniques were utilised for construction of the toggle switch.

Golden Gate assembly (Figure 11) is a cloning method which exploits the enzymatic properties of Type II restriction endonucleases and T4 DNA ligase to join multiple DNA fragments into a single DNA part, simultaneously and unidirectionally. Type II restriction enzymes recognise 6bp nonpalindromic sequences and cleave DNAs outside of these recognition sequences, resulting in unique 4bp overhangs (single stranded DNA). These overhangs are used as the fusion sites, and directionality is maintained as a result of 3' fusion site of the upstream part complementing the 5' fusion site of the following. The resulting overhangs on adjacent DNA fragments anneal, and are joined together using T4 DNA ligase to form a transcriptional unit (TU) (Figure 12). A typical assembly produces a transcriptional unit with four parts (promoter, ribosome binding site, coding sequence, and terminator) assembled into a backbone – usually a DVK (kanamycin-resistance) destination vector or DVA (ampicillin resistance) destination vector).<sup>[24]</sup>

## *E. coli* Modular Parts and Vectors

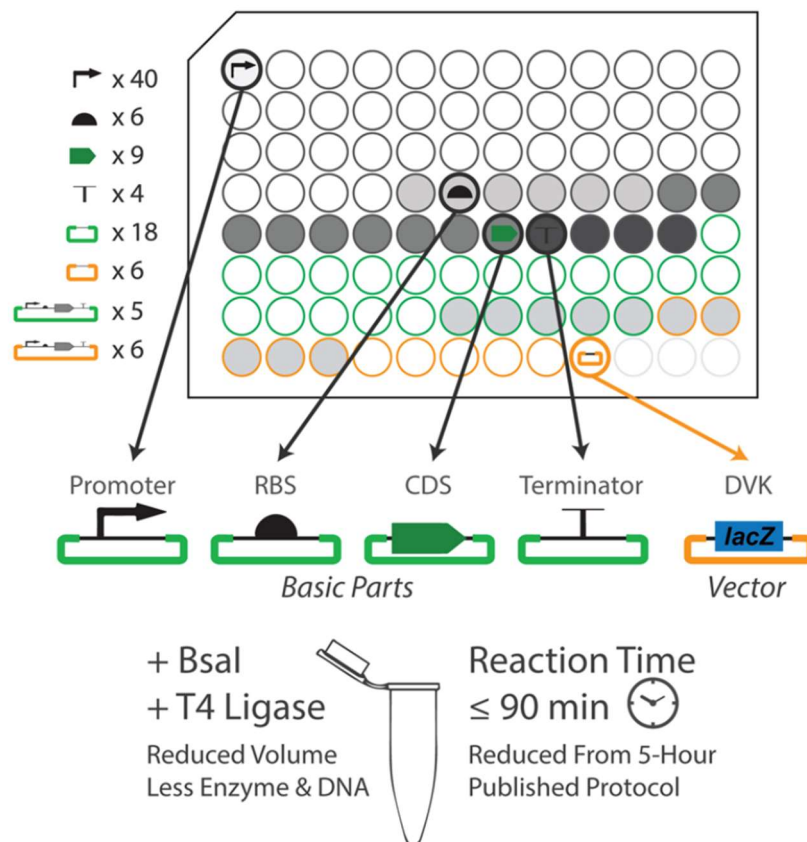
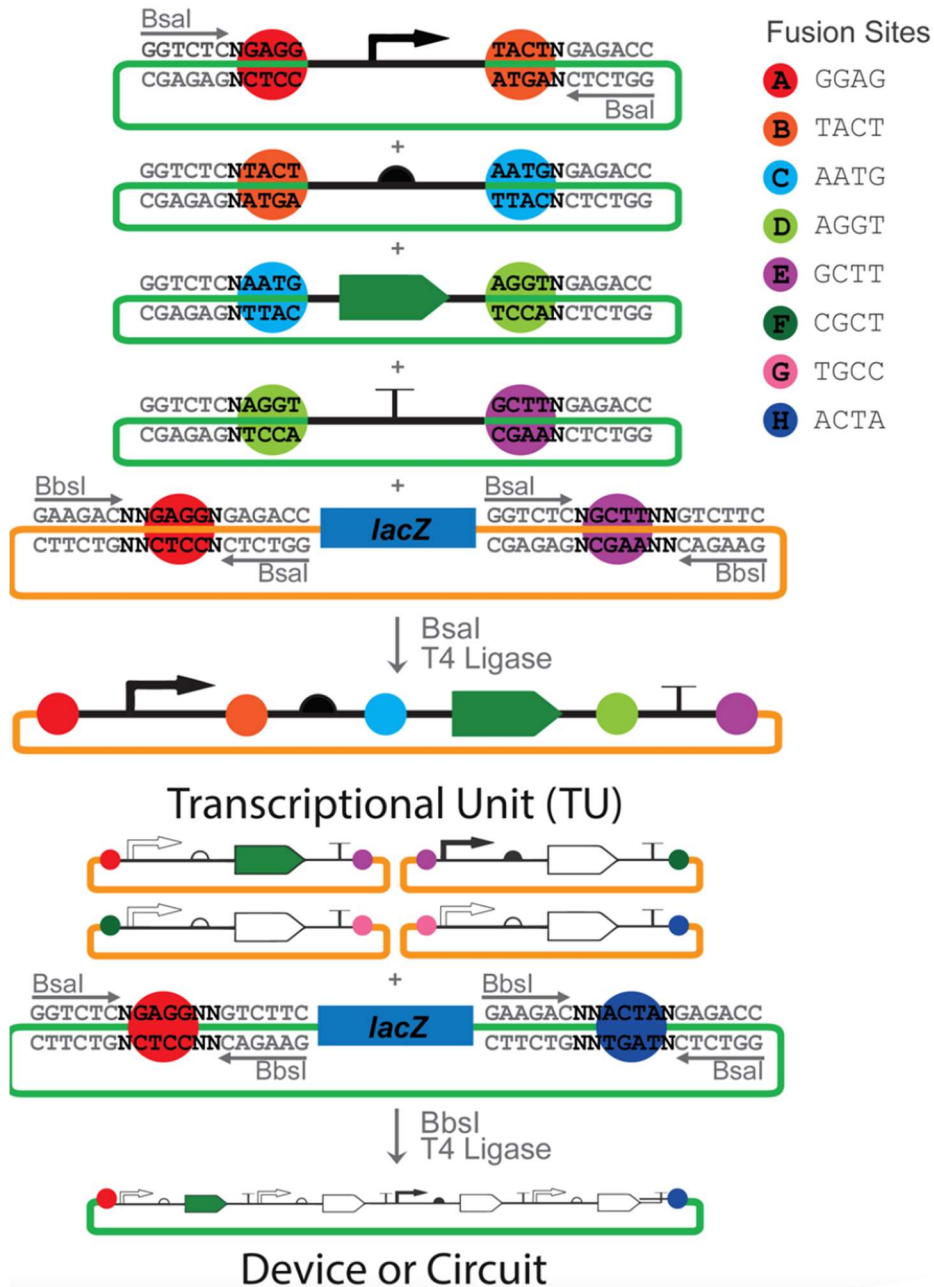


Figure 11. *E. coli* modular parts on the 96 wells plate and destination vectors<sup>[24]</sup>

# CIDAR MoClo Assembly Format



**Figure 12.** Shows level of assembly in CIDAR MoClo from individual DNA parts to a single TU and lastly a device [24]

Gibson assembly (Figure 13) allows the joining of multiple DNA fragments (up to 15 pieces) in a single, isothermal reaction using exonucleases, DNA polymerase, and DNA ligase. Adjacent DNA fragments must overlap by 20-40bp in order to ensure successful assembly. The exonuclease cleaves DNA from the 5' end, exposing complementary ssDNA. Resulting ssDNA sections on neighbouring DNA fragments can anneal, with the DNA polymerase incorporating nucleotides to fill spaces, which are subsequently covalently joined by DNA ligase. [25]

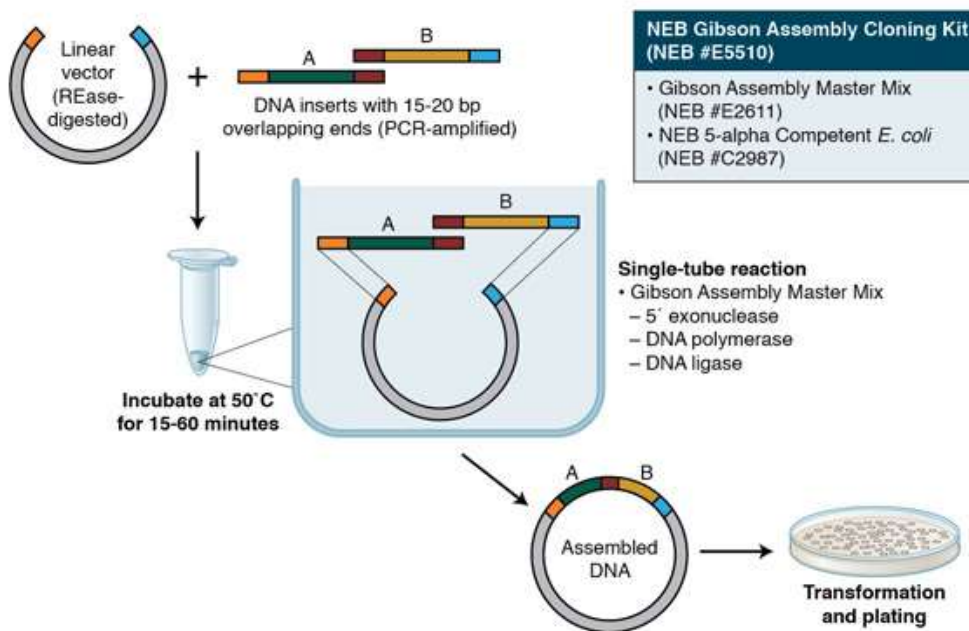


**Figure 13.** Gibson Assembly Overview [25]

Comparison of the characteristics of the two assembly methods:

Golden Gate Assembly	Gibson's Assembly
<ul style="list-style-type: none"> <li>• Parts need to be flanked by sites for BsaI cutting and can't contain BsaI sites</li> <li>• Need 4 base 'scars' between parts</li> <li>• Thermocycler is required for reactions</li> <li>• Parts need to be housed in 'part plasmids' before they can work</li> </ul>	<ul style="list-style-type: none"> <li>• Don't need to worry about the restriction enzyme sites</li> <li>• No 'scar' bases left between parts</li> <li>• Easy reaction for the user</li> <li>• Parts to assemble can be provided Straight from a PCR reaction</li> </ul>
<ul style="list-style-type: none"> <li>• Works very efficiently regardless of part sequence and how long the part is</li> <li>• Very good modularity so it is useful for making combinatorial libraries.</li> </ul>	<ul style="list-style-type: none"> <li>• Assembly works badly for repetitive sequences (e.g. terminators) and not at all for small parts (e.g. RBS)</li> <li>• Lack of modularity so not suitable for combinatorial work, only good for one-time design</li> </ul>

**Table 3.** Advantages and disadvantages of Golden Gate vs Gibson's Assembly [26]

## 5.2 *In silico* assembly (Benchling)

Due to the unpredictable nature of molecular cloning techniques, two methods were pursued in tandem to increase probability of success.

### 5.2.1 Method 1: Golden Gate Only Assembly

Figure 14 shows an overview of the Golden Gate Assembly method. DNA parts are placed into destination vectors (with 4 parts per backbone) to form four transcription units (TUs) - GGO\_A, GGO\_B, GGO\_C, and GGO\_D. Subsequently these four plasmids are assembled into backbone of DVK\_AH to construct the whole toggle switch plasmid GGO\_E. Each circle represents unique complementary overhanging sequences between adjacent parts.

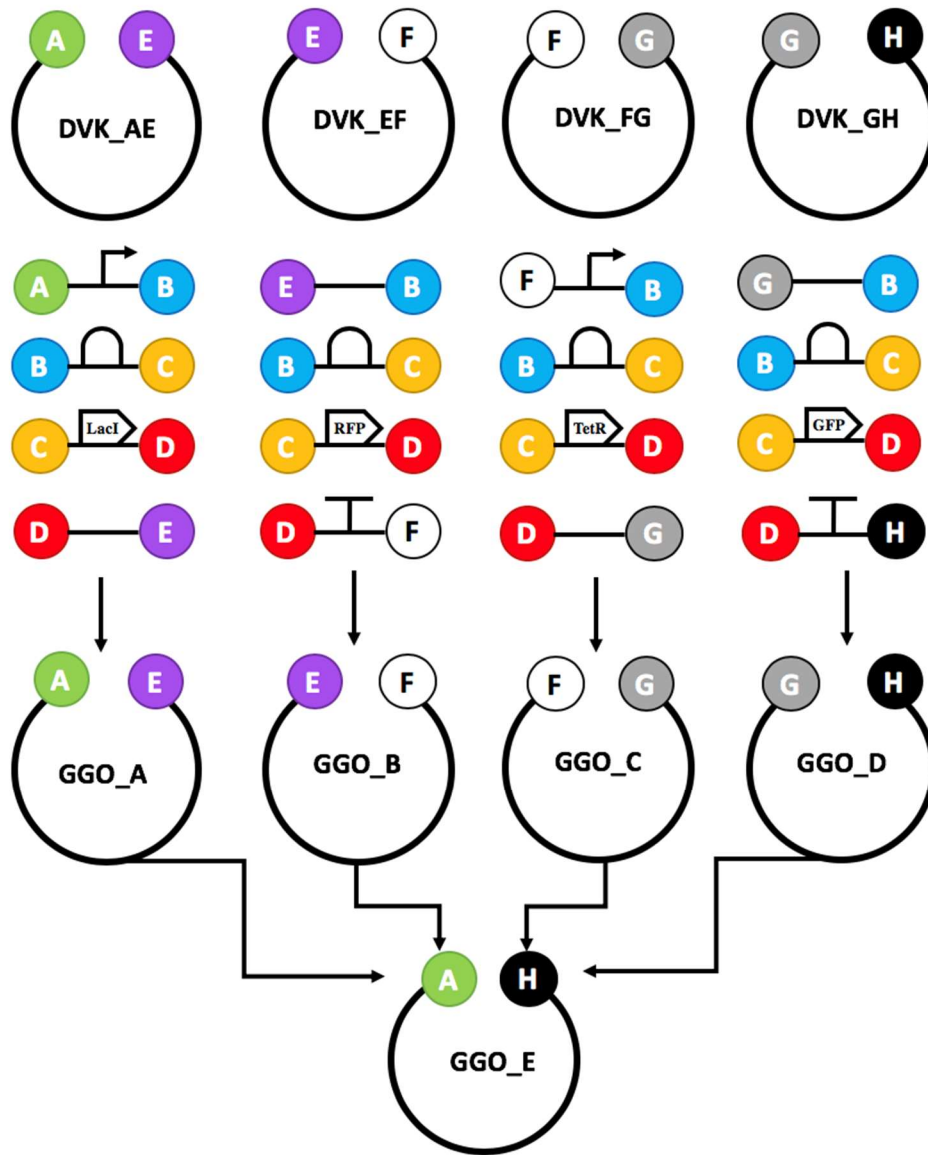


Figure 14. Overview of Method 1, using Golden Gate Cloning Assembly

### Step 1: Spacer creation

Four new spacers were created manually. They were necessary for the correct ligation of consecutive parts. A specific sequence for the overhangs on either side of the spacer can be generated, so spacers (*Figure 15*) can be used to link two parts that do not have complementary overhangs together.

<b>Spacer EB</b> CGCTTCACTGTCAGGTA ACTA GCGAAGTGACAGTCCATGAT Spacer EB	<b>Spacer DE</b> ;CAGGTTGACATCTGGGCTTA  GTCCA ACTGTAGACCCGAAT Spacer DE
<b>Spacer DG</b> ;CAGGTTGCGTTCTTCTGCCA  GTCCAACGCAAGAAGACGGT Spacer DG	<b>Spacer GB</b> CTGCCCCGTGGTCAAATACTA GACGGGCACCAGTTTATGAT Spacer GB

*Figure 15.* The sequences of the spacers used

### Step 2: Construction of GGO\_A, GGO\_B, GGO\_C and GGO\_D

All constituent plasmids were created by *in silico* assembly of BioBricks. A schematic of each plasmid was made, showing their backbone and constituent parts. (*Figure 16*)

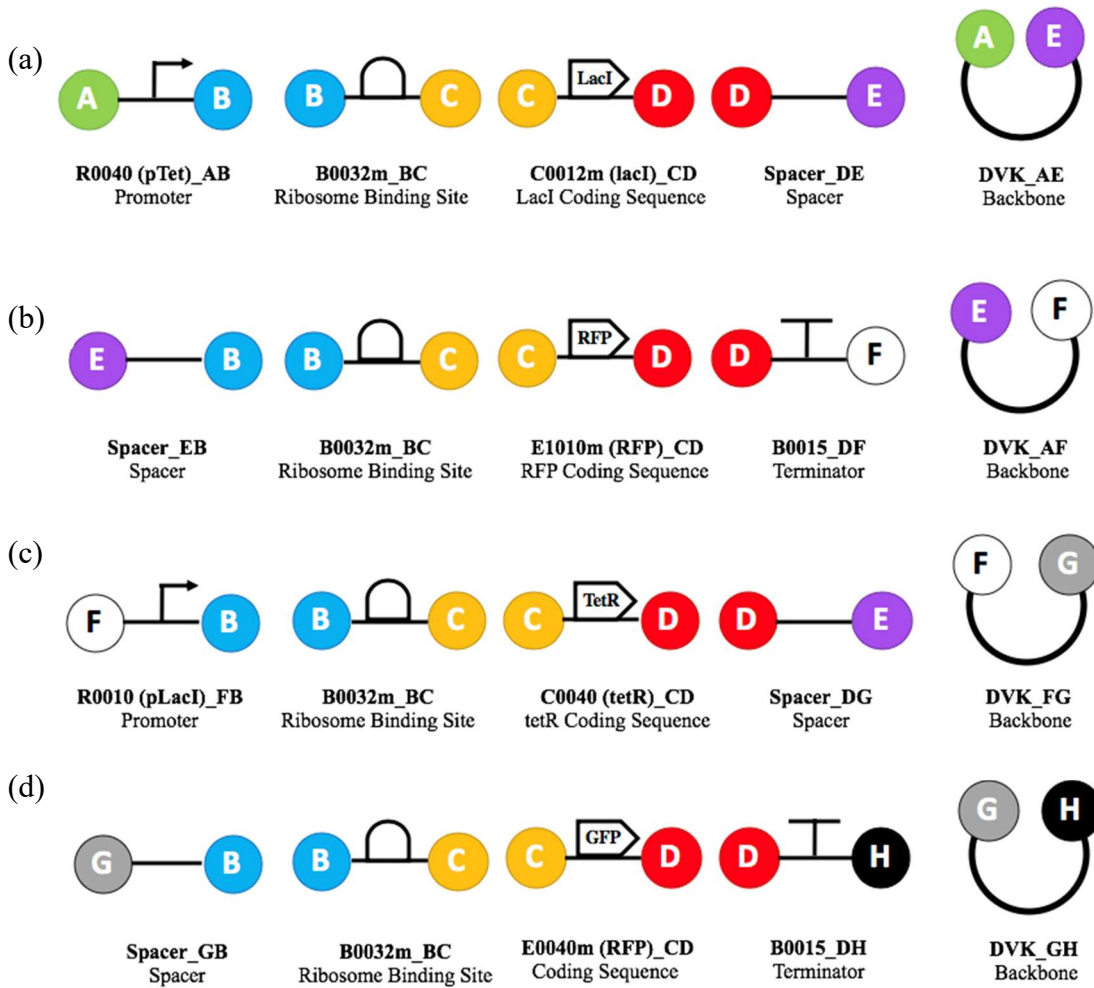


**Figure 16.** Constituent backbone parts of each plasmid, and the type of BioBrick

These parts were assembled *in silico* via simulated Golden Gate Assembly on Benchling. The finished products, Plasmids GGO\_A to GGO\_D are shown in *Figure 17*.

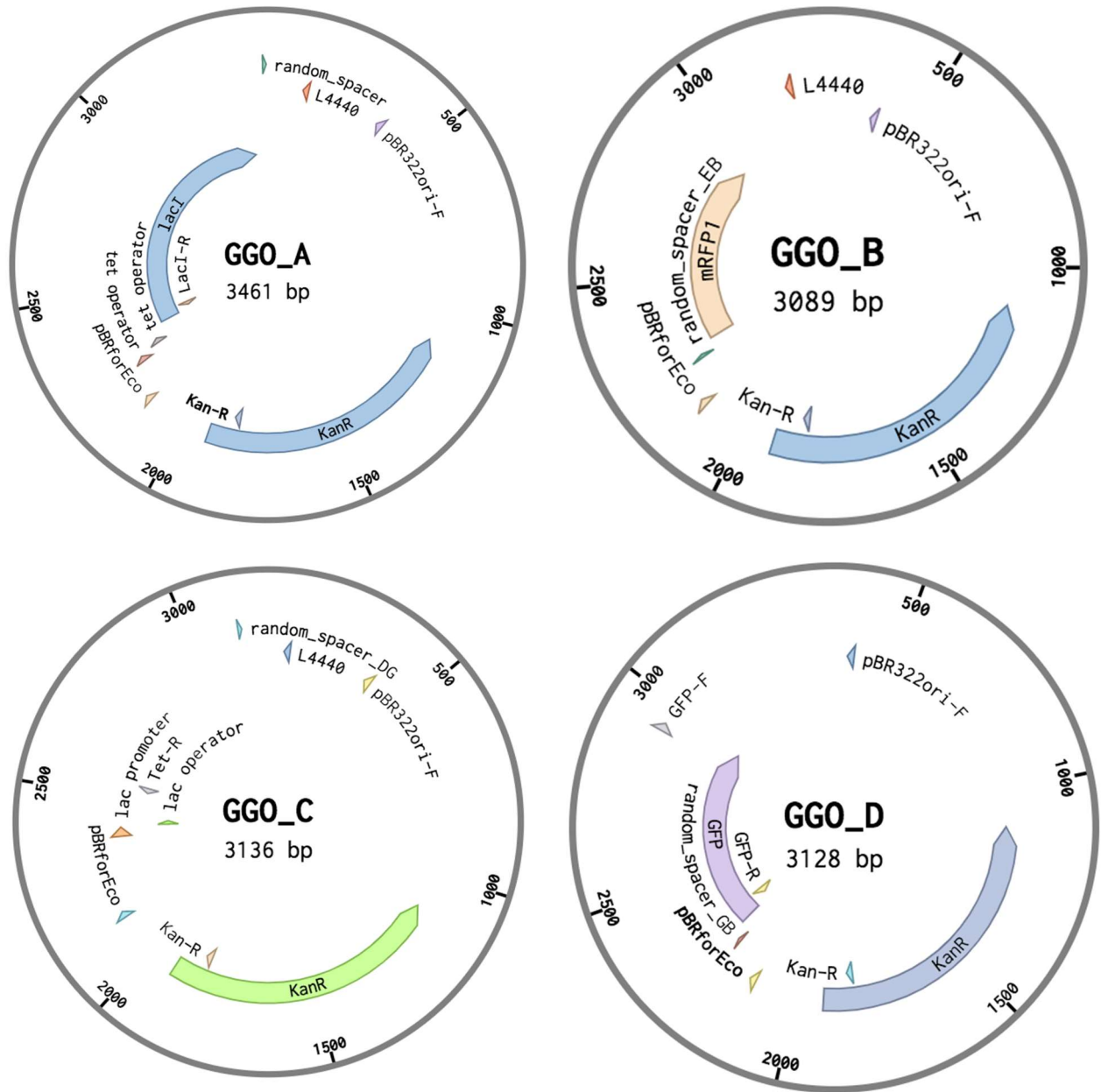


Figure 17. *In silico* representation of the constituent parts of Plasmid GGO\_E – Plasmid GGO\_A, GGO\_B, GGO\_C and GGO\_D

Step 3: Construction of GGO\_E

GGO\_E (Figure 18) is the final toggle switch construct. To ensure successful directional assembly, adjacent plasmids have unique complementary bases present on their overhangs. (Figure 19).

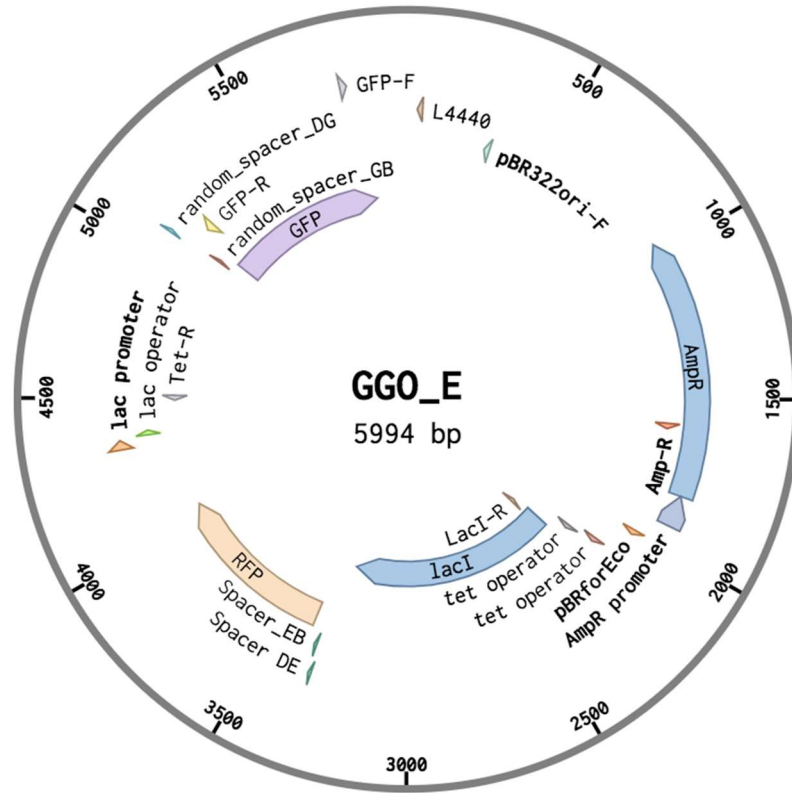


Figure 18. *In silico* representation of Plasmid GGO\_E.

Upstream	Downstream	Bases <span style="color: blue;">i</span>	Reverse Complement
DVA_AH	GGO_A	ggag	ctcc
GGO_A	GGO_B	GCTT	AAGC
GGO_B	GGO_C	cgct	agcg
GGO_C	GGO_D	TGCC	GGCA
GGO_D	DVA_AH	acta	tagt

Figure 19. Constituent parts of Plasmid GGO\_E and the complimentary overhangs between them.

### 5.2.2 Method 2: Golden Gate and Gibson Assembly

Figure 20 shows an overview of the Golden Gate and Gibson assembly method. DNA parts are placed into two destination vectors (with 4 parts per backbone) to form two transcription units (TUs) using Golden Gate assembly - GGG\_A, and GGG\_B. Subsequently these are used to form GGO\_C and GGO\_D, which in turn make up GGO\_E which contains the whole toggle switch construct.

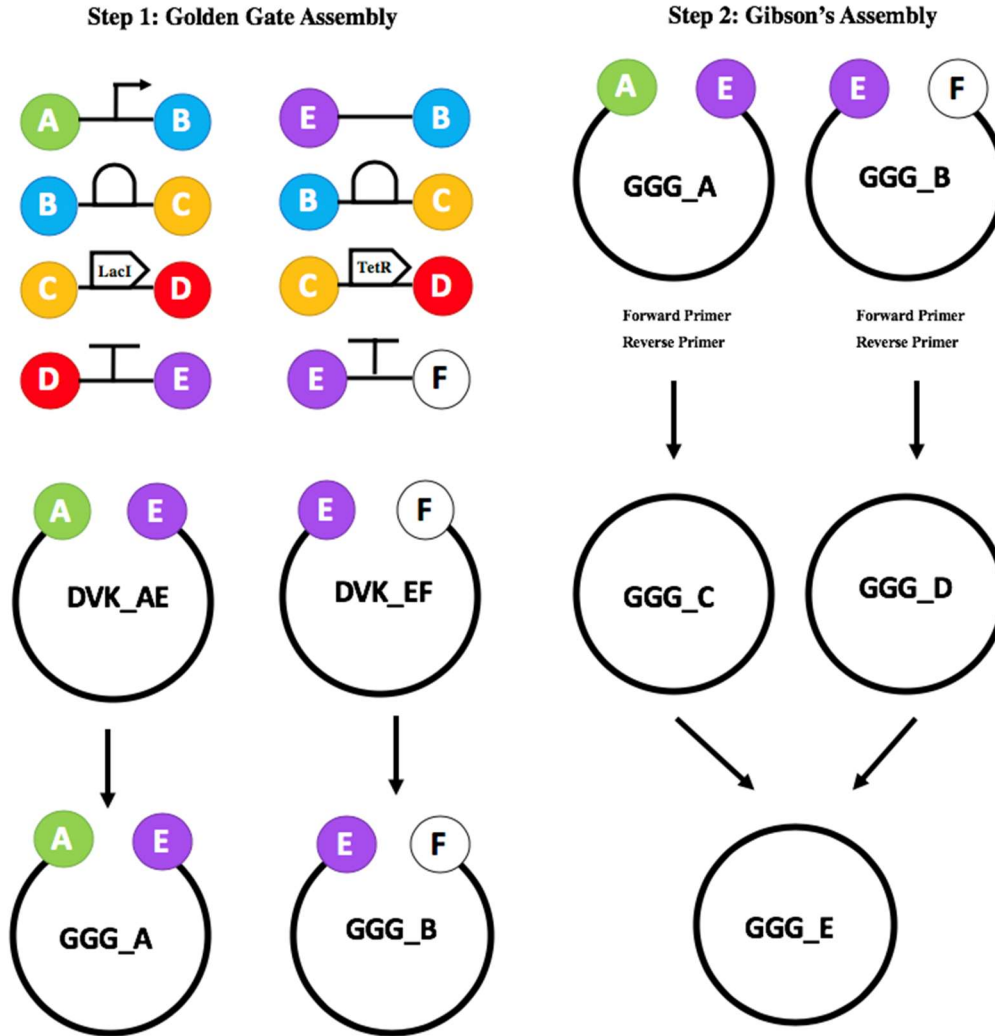
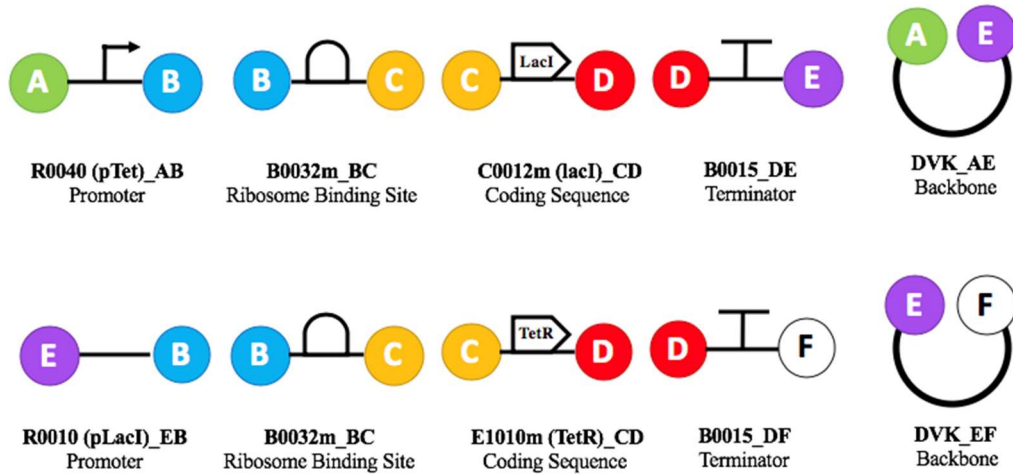


Figure 20. Overview of Method 2, using Golden Gate Cloning and Gibson's Assembly.

**Step 1: Construction of GGG\_A and GGG\_B (via Golden Gate Assembly)**

Constituent parts (Figure 21) were assembled via simulated *in silico* Golden Gate Assembly to construct plasmids GGO\_B and GGO\_A (Figure 22).



**Figure 21.** Constituent parts of GGG\_A and GGG\_B

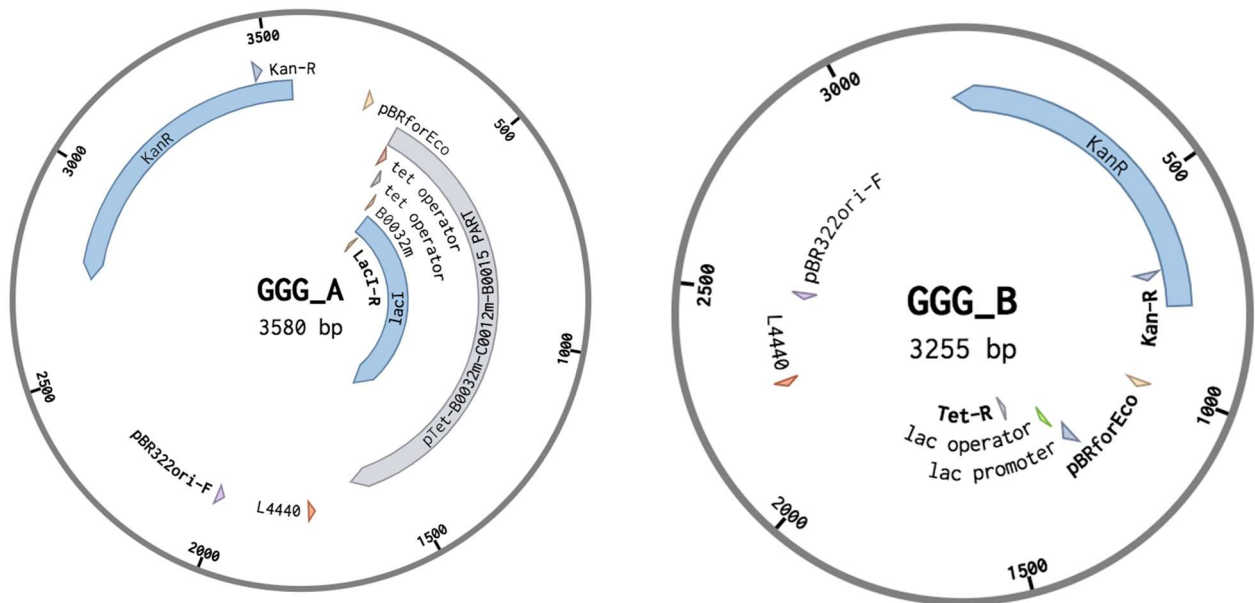


**Figure 22.** *In silico* schematic of plasmids GGG\_A and GGG\_B.

### Step 2: Construction of GGG\_C and GGG\_D (via Gibson Assembly)

Subsequently, virtual Gibson's assembly was used to linear fragments were created from GGG\_A and GGG\_B using PCR, which formed plasmids GGG\_C and GGG\_D (Figure 23). The primers used for this reaction (Appendix C) was designed by Benchling according to strict parameter (Appendix C)

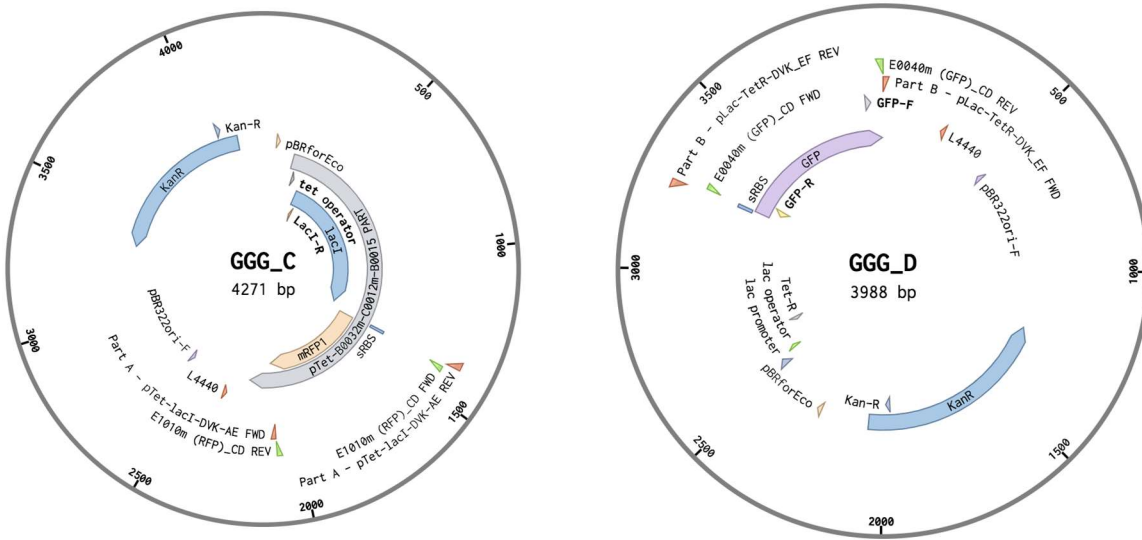


Figure 23. In silico schematic of plasmids GGG\_A and GGG\_B.

### Step 3: Construction of GGG\_E (via Golden Gate Assembly)

GGG\_E (Figure 24) is the final toggle switch construct. To ensure successful directional assembly, adjacent plasmids have unique complementary bases present on their overhangs. (Figure 25).

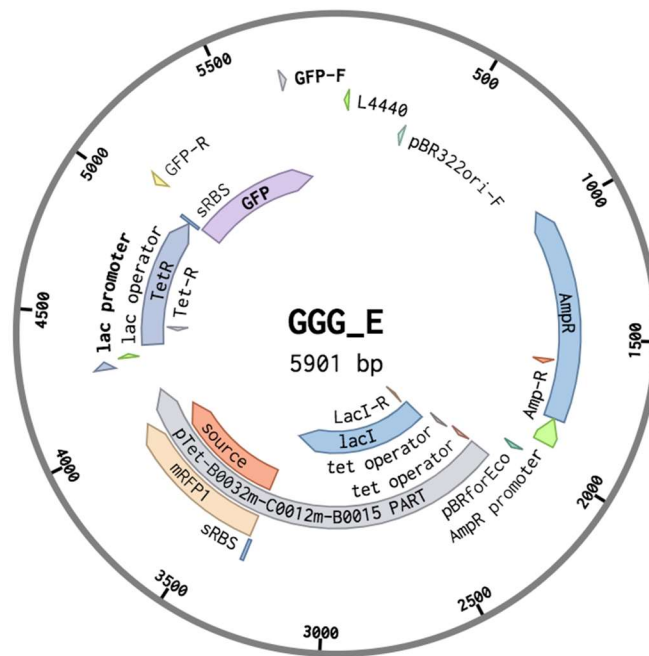


Figure 24. In silico representation of Plasmid GGG\_E

Upstream	Downstream	Bases <span style="color: blue;">i</span>	Reverse Complement
DVA_AF	GGG_C	ggag	ctcc
GGG_C	GGG_D	gctt	aagc
GGG_D	DVA_AF	cgct	agcg

**Figure 25.** Constituent parts of Plasmid GGG\_E and the complimentary overhangs between them.

### 5.3 Methods and Protocols (*in vitro* assembly)

#### DNA Cloning and assembly:

Parts for GGO\_A, GGO\_B, and 2 types of fluorescent proteins for controls were ordered from Addgene (*Appendix D*). DNA parts were contained in *E. coli* cultures.

#### Cultivation of parts on Agarose Gel

Different colonies of *E. coli* containing the DNA parts were streaked onto pre-prepared agarose plates. Plates were inoculated at 37C. (*Appendix E1 and E2*)

#### DNA Extraction and Purification

Each *E. coli* culture was extracted, and the plasmid DNA is purified. Protocol (*Appendix E3*) and reagents from the QIAGEN Spin Miniprep kit (*Figure 26*) were used.

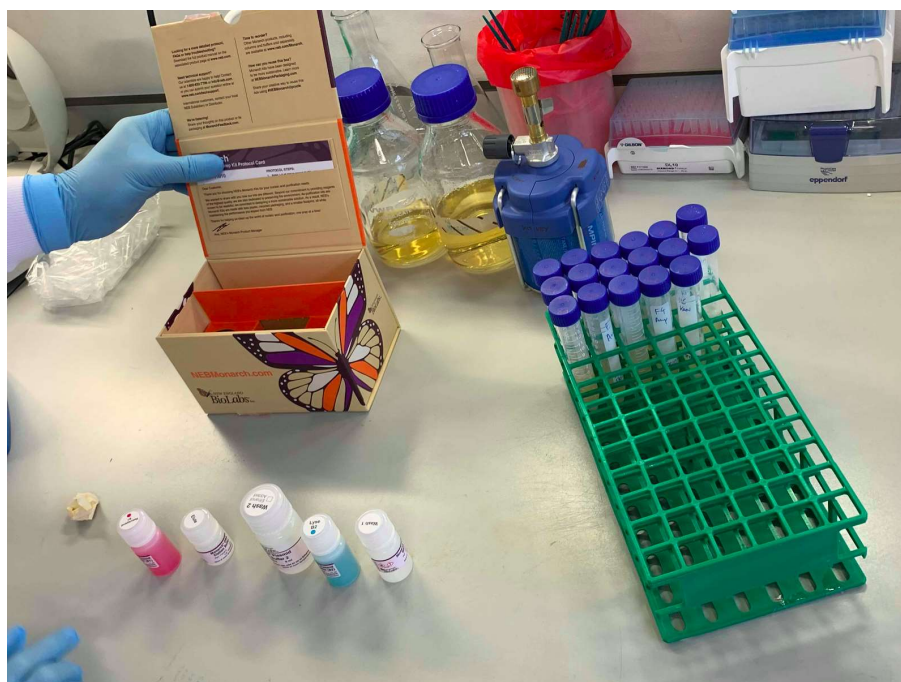


**Figure 26.** Contents of the QIAGEN Spin Miniprep kit

### Primer creation (Protocol 4 and 5)

Spacers DE and EB were ordered as oligonucleotides (primers). The primers were 5' phosphorylated (*Appendix E4*) and annealed together (*Appendix E5*) to create dsDNA parts.

### Molecular Cloning

Golden Gate Assembly (*Appendix E6*) and Gibson's Assembly (*Appendix E7*) were used to assemble DNA parts together

### Transformation

Heat Shock Protocol (*Appendix E8*) was used on each plasmid and *E. coli* (strain DH5 $\alpha$ ) to transform them into chemically competent cells containing the toggle switch plasmid. Blue-white screening was used to confirm successful transformation.

### Plasmid Verification and Sequencing

Another miniprep (*Appendix E3*) was done to extract and purify the plasmids from successful colonies, and the DNA sequences sent for sequencing, and compared with *in silico* models. Primer sequences can be found in *Appendix F*

### PCR and Gel Electrophoresis

PCR (*Appendix E9*) was used to amplify 2 DNA parts for Gibson assembly of plasmid GGG\_D. Gel electrophoresis (*Appendix E10*) was used to visualise fragments. Fragments were loaded into the agarose gel containing SYBR® Safe DNA Gel Stain with Hyderladder 1kb as reference. The gel is run for 1.5 hours at 100V, then visualised under UV light.

## 5.3.2 Analysis of chassis compatibility

*E. coli* containing toggle switch constructs were cultured, and toggle switch plasmids were extracted and purified using the protocol and reagents from the QIAGEN Miniprep Spin Kit. The chassis to be tested ( $\Delta$ lacI/ $\Delta$ araC *E. coli* cells) were also cultured and transformed into chemically competent cells. The purified toggle switch constructs were then transformed into the competent  $\Delta$ lacI/ $\Delta$ araC *E. coli* cells, and this was cultured.

A plate reader assay was conducted in order to evaluate chassis compatibility in BL21 and  $\Delta$ lacI/ $\Delta$ araC *E. coli* strains. The cultures and inducers were transferred to their respectable wells. The plate reader was programmed to measure absorbance at 600nm wavelength every 11 minutes for 9 hours. The excitation wavelengths were set at 485 and 590nm, and emission wavelengths were set at 528 and 645nm for measuring GFP and RFP respectively. For an exhaustive list of all experiments see *Appendix G*.

The expected results are as follows:

- No inducer: Constitutently expresses GFP
- IPTG: Transition to RFP<sup>+</sup>/GFP<sup>-</sup> state
- Arabinose: transition to an RFP<sup>+</sup>/GFP<sup>-</sup> state\* due to induced expression of mflon protease
  - o pECJ3 + pZA16mflon: fast rate of switching
  - o pECJ3B + pZA16mflon: decreased rate of switching due to weaker degradation tag
  - o pECJ3D + pZA16mflon: even more decreased rate of switching due to even weaker degradation tags<sup>[27]</sup>

## 6. Experimental Results

### 6.1 GGG\_B Plasmid Verification and Sequencing

Sequencing data confirms experimental construct matches the *in silico* design for plasmid GGG\_B (Figure 27), therefore *in vitro* construction was successful. Vertical red bars represent a potential mismatch (e.g. a deletion or an incorrect base) with the target sequence, whilst grey areas represent correct base sequence. Figure 28 shows a close-up of the experimental base sequence compared to the predictions, as well as the quality of the data.

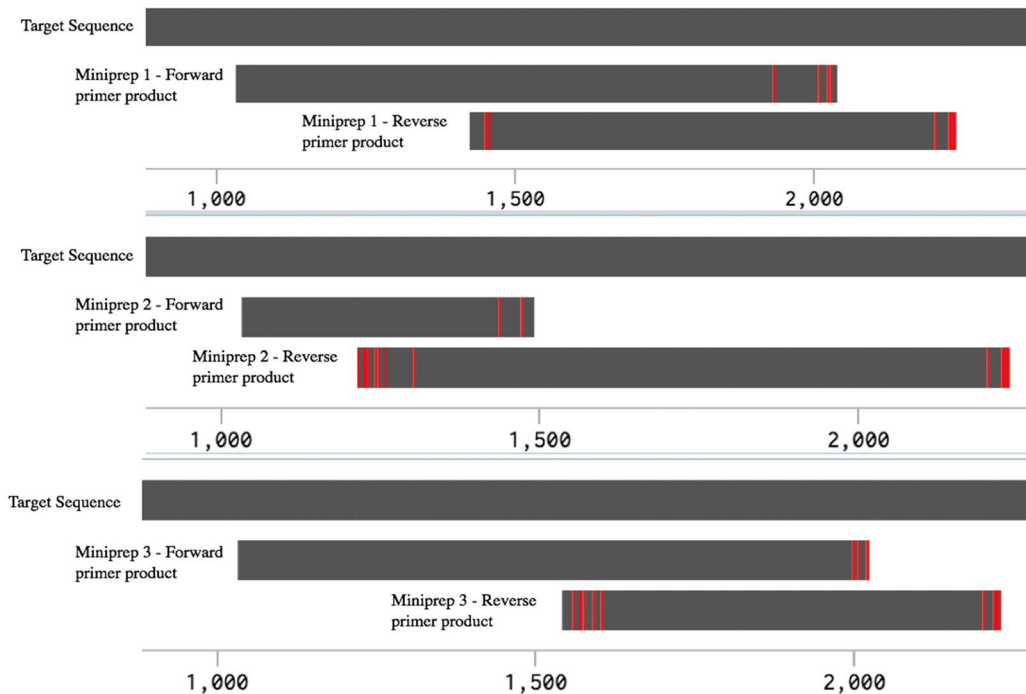


Figure 27. Alignment analysis data for 3 minipreps of plasmid GGG\_B.

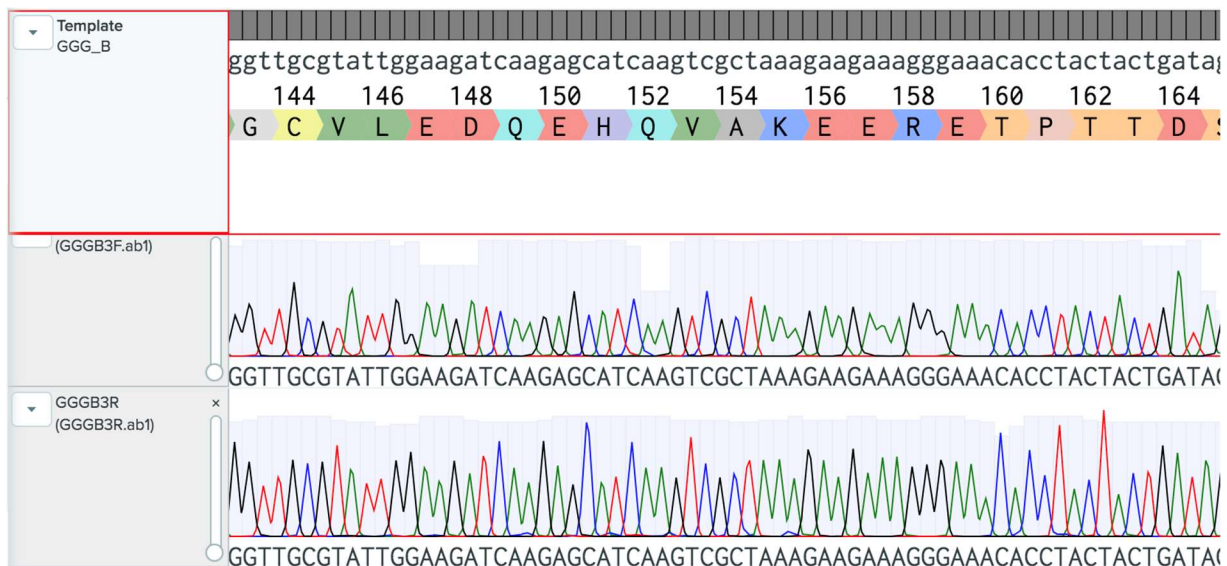


Figure 28. Close-up of analysis of 3 miniprepped constructs.

A band at 3-4kBP was expected in lane 2 and 3 according to Benchling predictions, however this was not present. A band at 700BP was expected and present, implying successful isolation of the smaller fragment. (Figure 29 and Table 11)

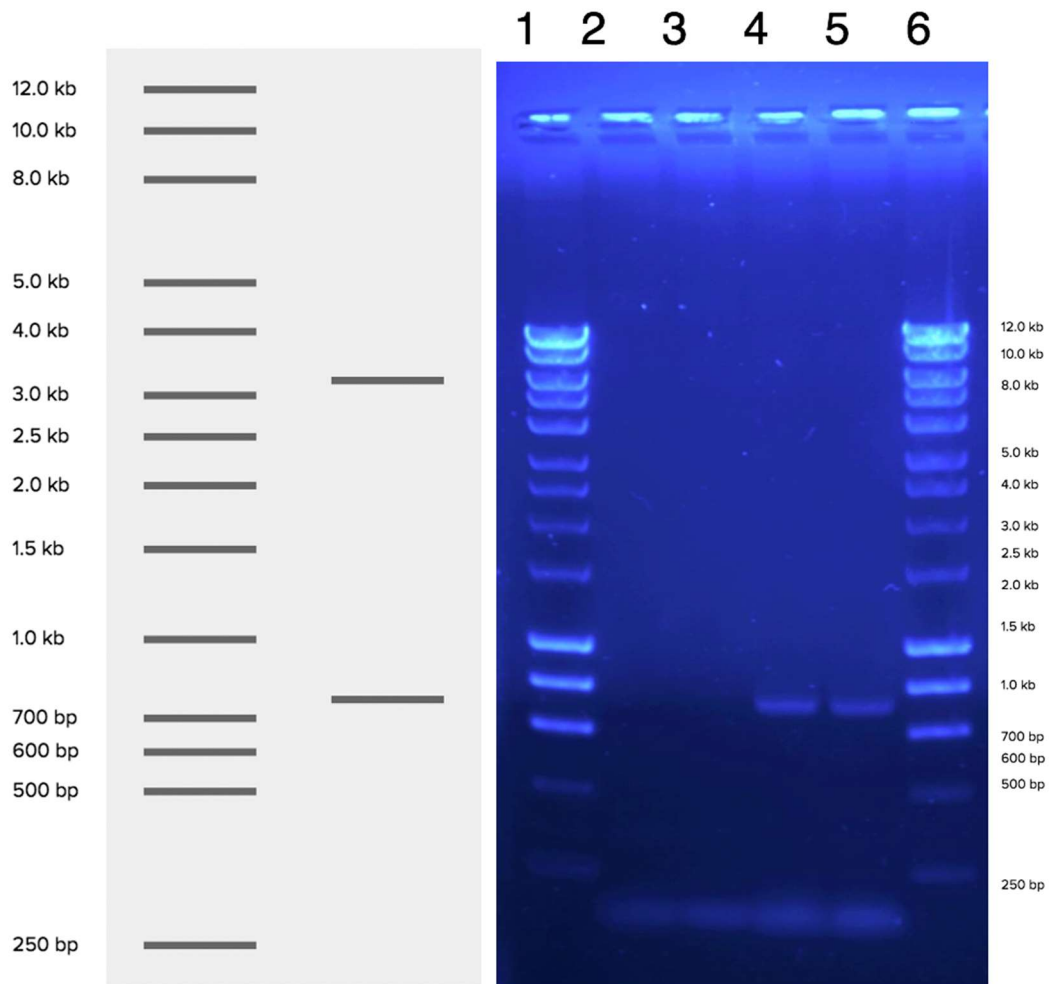


Figure 29. Gel electrophoresis (R) to validate constructs, compared against the *in silico* prediction (L)

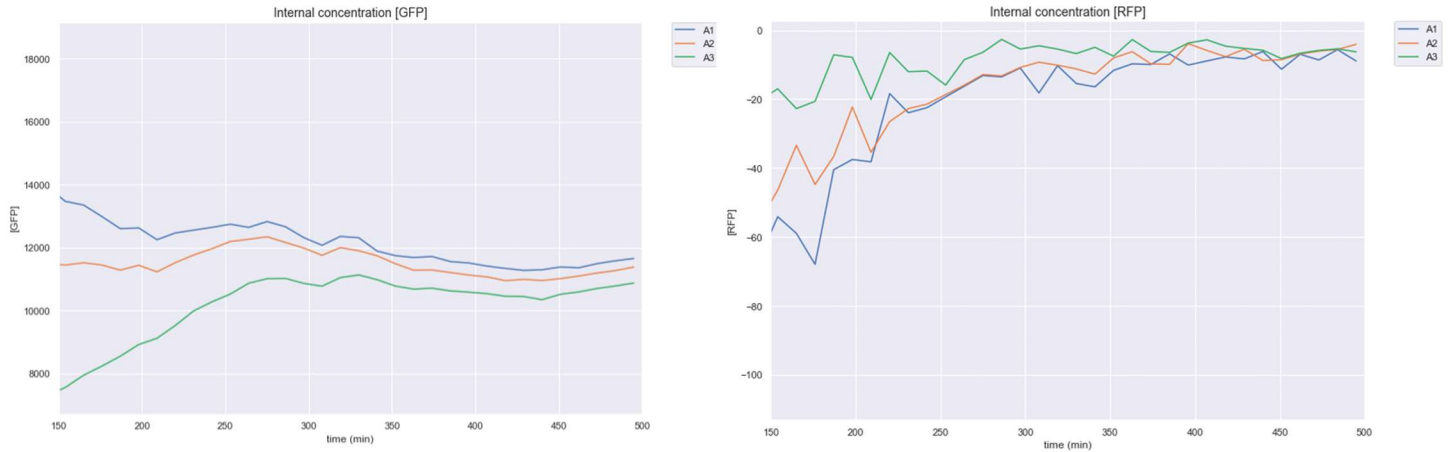
LANE	CONTENTS	RESULT
1	Bioline Hyderladder 1kb Plus	Reference Ladder
2	3-4kb fragment amplified with HF Buffer	Unsuccessful
3	3-4kb fragment amplified with GC Buffer	Unsuccessful
4	700bp fragment amplified with HF Buffer	Successful
5	700bp fragment amplified with GC Buffer	Successful
6	Bioline Hyderladder 1kb Plus	Reference Ladder

Table 11. Gel electrophoresis Well Contents and Results

## 6.3 Tests of chassis compatibility:

### 6.3.1 Controls

Despite having different starting concentration of GFP expressed, the GFP levels are constitutively expressing. The 3 tests were concordant as they reached the expression level of around 11000.



*Figure 30. Control 1: No inducer added*

Upon addition of inducer IPTG, the level of GFP expression reaches a level of 10500 as it levels out after 250mins. We expect there to be no inducer effect. If we do not consider the starting concentration and the level of expressive is similar to that of no inducer, thus the test is successful.

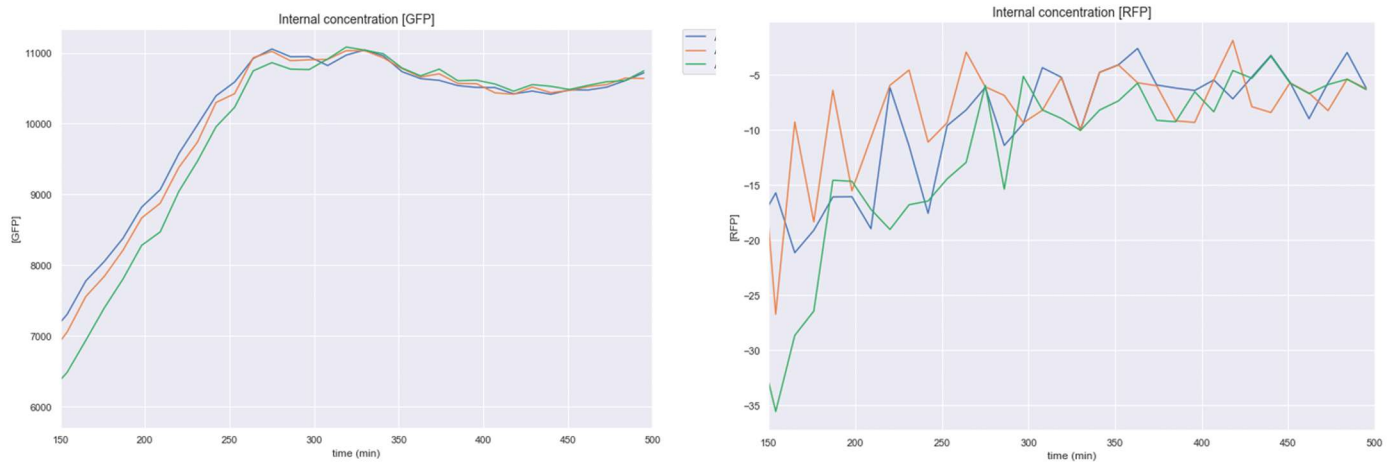


*Figure 31. Control 2: IPTG inducer added.*

Upon addition of inducer arabinose, the level of GFP expression reaches a level of 10000 at time 350mins. The blue line however is a faulty result because the GFP expression level is lower than the other 2 lines. The tests indicated by green and orange lines are successful.

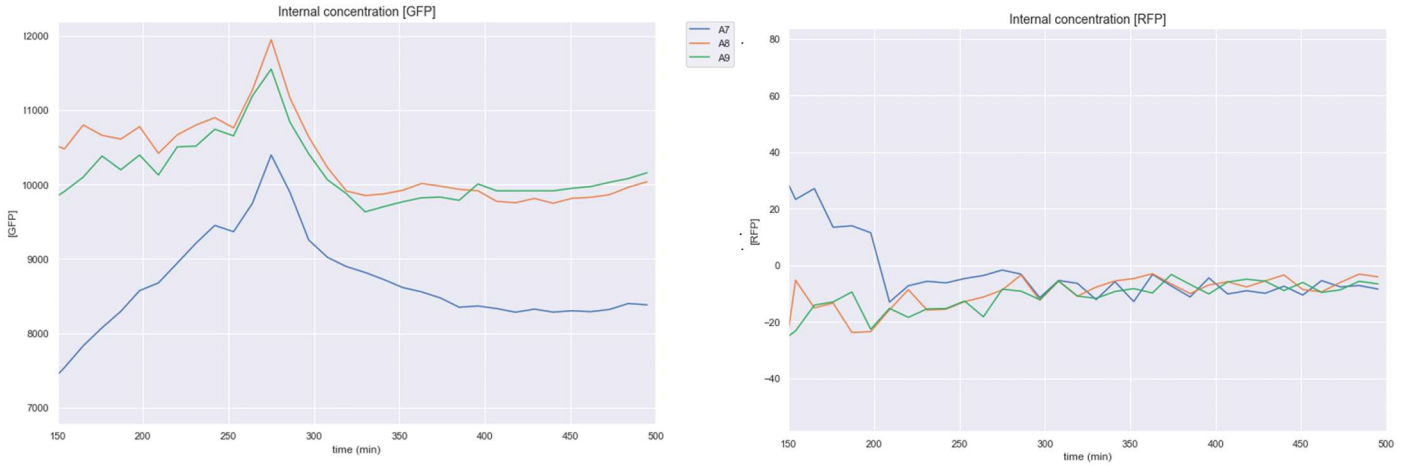


Figure 32. Control 3: Arabinose inducer added.

### 6.3.2 pECJ3B + pZA16mflon in $\Delta$ lacI/ $\Delta$ araC *E. coli*

Without inducers added, the GFP expression levels were high, at around 2000-6000 arbitrary units. RFP expression levels were low, at around -20 to 20 arbitrary units. (Figure 33)

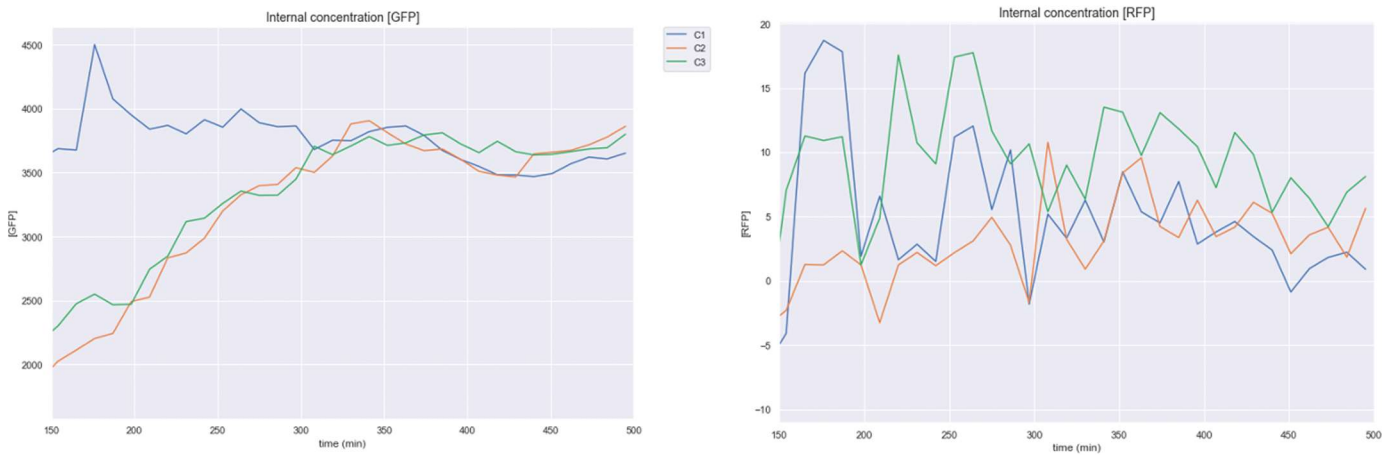
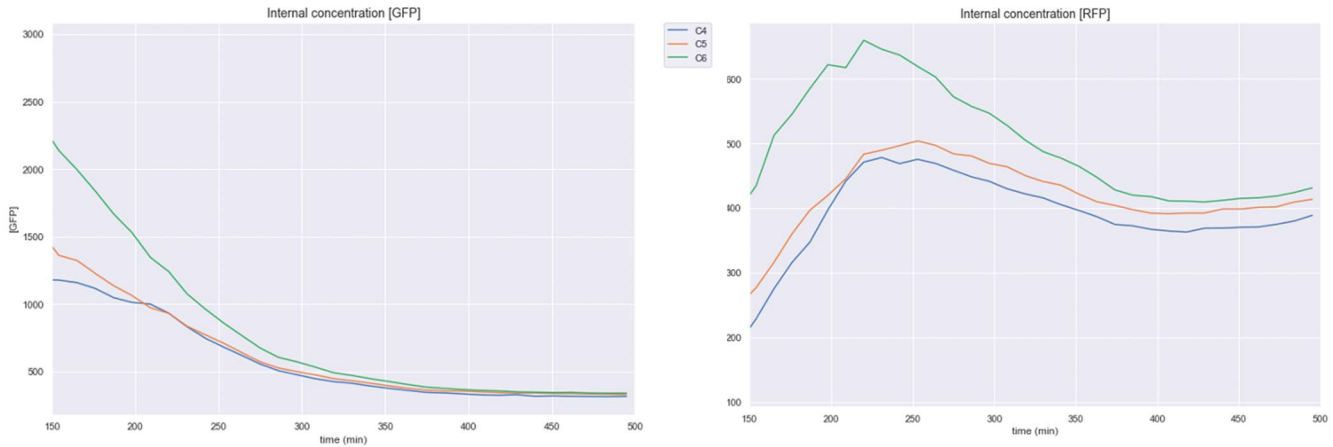


Figure 33. Baseline GFP/RFP expression in  $\Delta$ lacI/ $\Delta$ araC *E. coli* with pECJ3 + pZA16mflon toggle switch; no inducers added.

Upon addition of inducer IPTG, GFP expression decreased to 1000 arbitrary units or less, and RFP expression levels increased to around 800 arbitrary units.



**Figure 34.** GFP/RFP expression in  $\Delta lacI/\Delta araC$  *E. coli* with pECJ3pECJ3B + pZA16mflon toggle switch after IPTG induction

Upon addition of inducer Arabinose, low to high switching occurred – GFP levels converge to around 4000-5000 arbitrary units, and RFP levels decreased to around 5 arbitrary units.

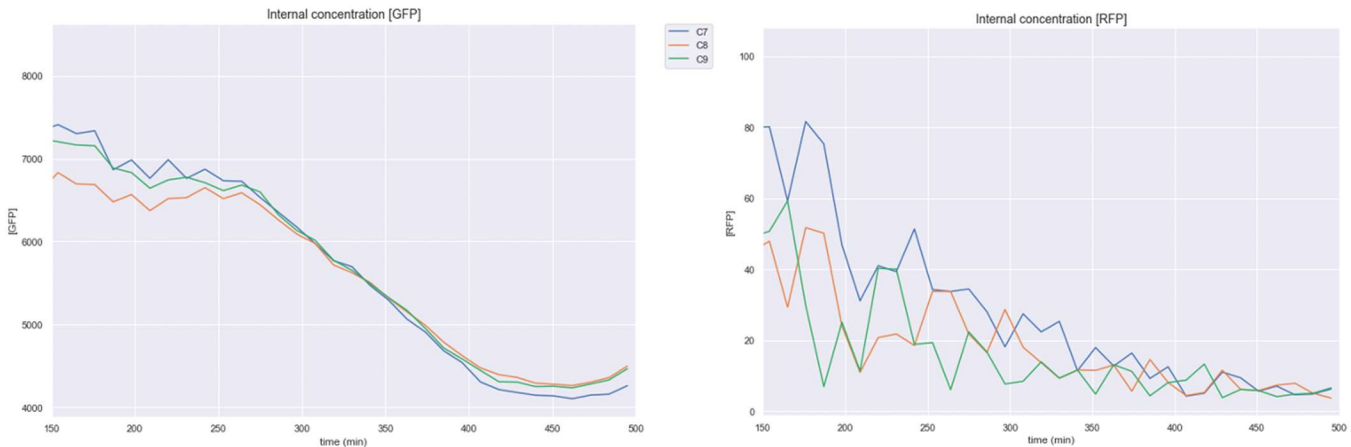


**Figure 35.** GFP/RFP expression in  $\Delta lacI/\Delta araC$  *E. coli* with pECJ3 + pZA16mflon toggle switch after Arabinose induction

There is some evidence that the toggle switch reached 2 distinct steady states:

- In the presence of IPTG, GFP levels are low and RFP levels are high
- In the presence of IPTG, GFP levels are low and RFP levels are high

Therefore, the toggle switch pECJ3B + pZA16mflon was successful and compatible with the  $\Delta lacI/\Delta araC$  *E. coli* chassis

## 7. Discussion

All toggle switches tested in the different chassis were successful to varying degrees (Appendix H). Successful toggle switches have 2 distinctive stable states, with a large dynamic range. Using this definition, pECJ3 + pZA16mflon construct in the was successful and compatible with the  $\Delta$ lacI $\Delta$ araC Chassis, as it achieved a dynamic range of 4.5-fold in GFP (levels were 4500 arbitrary units when high and 1000 when low) and 160-fold in RFP (levels were 800 when high and 5 when low). One original limitation of Gardner's pTAK toggle switches is the imbalance in switching time (6 hours to achieve the high state, 30 minutes to achieve the low state)<sup>[1]</sup>. The toggle switches tested in this report were generally able to achieve a more balanced switching time (5 hours from low to high, and 5 hours from high to low).

Toggle switches tested in a new chassis (BL21) were found to be less successful in general compared to when they were implemented in a tested strain  $\Delta$ lacI $\Delta$ araC – therefore they were less compatible with this chassis.

In some cases, switching occurred slowly (in the pECJ3B + pZA16mflon, and pECJ3D + pZA16mflon toggle switches) and GFP/RFP expression levels were often fluctuant. This might be due to the fact that pZA16mflon toggle switch constructs contain the original mf-lon cassette, which is not codon optimised for expression in *E. coli*. Furthermore, weaker degradation tags construct may have led to a decrease in the rate of switching<sup>[27]</sup>. In future works, the duration of the experiments will be extended to reach a definitive conclusion on the success of these constructs.

There are several reasons that may have led to the unsuccessful assembly of plasmid GGO\_A *in vitro* despite successful *in silico* assembly in Benchling. First, reagents and DNA parts may have been contaminated with impurities, or the enzymes were potentially old which reduces their potency. Both of these contribute to decreases efficiency or unsuccessful cloning. The length of digestion time may also have been too short, so the reactions did not complete – this should be extended in future experiments. Furthermore, the *E. coli* may be limited in their competency, as it was the transformation part of the experiment which failed - more competent *E. coli* cells could be used in the future, including electrocompetent cells.<sup>[28]</sup>

Furthermore, working with living organisms leads to challenges due to evolution. Firstly, spontaneous mutations may occur, rendering the circuit redundant or less functional. Secondly, since the heterogenous components must compete with host processes for machinery and resources used in transcription and translation<sup>[20]</sup>, they may be rejected or expelled.<sup>[21]</sup> Thirdly, the parts may not be orthogonal, leading to unforeseen and unwanted interactions.<sup>[22]</sup> Therefore, *in silico* modelling is rarely replicated perfectly in the lab - despite extensive care used to minimise human error in the wetlab, the GGG\_B construct was not assembled successfully, although *in silico* assembly in Benchling was successful and predicted no errors.

## 8. Wiki

A comprehensive chronological account of our work can be found on our wiki - a website that serves as a digital logbook and contains extensive documentation on every aspect of the project, including our initial research, modelling and final implementation. The link to this is:

[https://openwetware.org/wiki/ICSynBio:GroupProj19\\_20](https://openwetware.org/wiki/ICSynBio:GroupProj19_20).

The screenshot shows a Wiki page with the following structure:

- Navigation:** Main Page, Recent changes, Help, Contact OWW, Add a Lab Notebook.
- Research:** Materials, Protocols, Resources.
- Search:** Search OpenWetWare, Go, Search.
- Tools:** What links here, Related changes, Special pages, Printable version, Permanent link, Page information, Cite this page.
- Page Content:**
  - Back, Project Home
  - Contents [hide]**
    - Toggle Switch Model Derivation
      - Chemical Reactions
      - ODEs of the system
      - Quasi-Stationary Approximation
      - Normalisation of the system
      - The system
    - Further Links
  - Toggle Switch Model Derivation**

The Model used by Gardner et Al to describe the genetic construct of the Toggle Switch can be derived from first principles.

**Chemical Reactions**

We start with the Chemical equations for Gene Expression (Central Dogma of Biology):

Protein A	Protein B
Transcription: $DNA \xrightarrow{k_{1,A} \cdot g(p_B)} DNA + mRNA_A$	Transcription: $DNA \xrightarrow{k_{2,B} \cdot f(p_A)} DNA + mRNA_B$
Translation: $mRNA_A \xrightarrow{K_2} mRNA_A + protein_A$	Translation: $mRNA_B \xrightarrow{K_2} mRNA_B + protein_B$
Degradation of mRNA: $mRNA_A \xrightarrow{d_1} \emptyset$	Degradation of mRNA: $mRNA_B \xrightarrow{d_1} \emptyset$
Degradation of protein: $protein_A \xrightarrow{d_2} \emptyset$	Degradation of protein: $protein_B \xrightarrow{d_2} \emptyset$

Some Assumptions we make are:

    - Transcription Rate can be given by following hill functions:
 
$$f(p_A) = \frac{K_{M,A}^{n_A}}{K_{M,A}^{n_A} + p_A^n}, \quad g(p_B) = \frac{K_{M,B}^{n_B}}{K_{M,B}^{n_B} + p_B^n}$$

$K_M = \text{repression coefficient}, n = \text{Cooperativity}$
    - The Translation Rate parameter is constant.
    - The mRNA and Protein degradation parameters are constant.

**ODEs of the system**

The Law of Mass Action allows us to yield the ODE's below that describe the rate of change of protein and mRNA concentration:

$$\frac{d[m]}{dt} = \dots - K_{..}^{nB}$$

Figure 36. Example of webpage from Project Wiki

## 9. Future Work

The current limitation of this project is that the theorised *in silico* toggle switch plasmids were unsuccessful *in vitro*. However, it is essential to gather data from wetlab experiments to compare them to the model prediction for the state of the system for each set of the parameters. Ideally, wetlab results should be used to feed back into another iteration of the design cycle. A new model of the toggle switch that includes the inducers will be derived. The appropriate choice of inducers has to be made and simulations of the inducer model with real parameters will be done. It is also necessary to validate the mathematical model of the toggle switch, by analysing other aspects of our mathematical model including accuracy and reusability.

The experiments testing toggle switches shall be extended to obtain more definitive conclusions about chassis compatibility. Upon completion of the toggle switch and its functionality testing, we aim to carry out RBS and promoter engineering of the toggle switch plasmid. This can be achieved by using site mutagenesis with the aid of Gibson's assembly.<sup>[31,32]</sup> The primers designed by Benchling will have single point mutations introduced to them, therefore promoting amplification of the plasmid with a mutated site. This allows a library of toggle switches to be built, with identical regulation yet different expression levels of protein.

In conclusion, we successfully constructed several constituent plasmids of a *de novo* working toggle switch, and tested 3 existing toggle switches for chassis compatibility with the  $\Delta$ lacI $\Delta$ araC and BL21 strains of *E. coli*, and characterised these constructs by *in silico* modelling. We conclude that the toggle switches were generally successful in  $\Delta$ lacI $\Delta$ araC *E. coli*. However, repeated testing with longer experiments are necessary to test compatibility with BL21 *E. coli*. Our next steps include completing the *de novo* toggle switch, subsequently create a library of toggle switches based on the initial construct using site mutagenesis, as well as repeating the testing of pre-existing toggle switch constructs with longer duration experiments.

## 10. References

1. Gardner, T., Cantor, C. & Collins, J. Construction of a genetic toggle switch in *Escherichia coli*. *Nature* 403, 339–342 (2000) doi:10.1038/35002131
2. Kitney R. *Synthetic Biology: Scope, Applications and Implications*; Royal Academy of Engineering: London, UK, 2009
3. G Baldwin, R Kitney, T Bayer et al. *Synthetic biology: A Primer*. London: Imperial College Press. 2016
4. Keshava, R., Mitra, R., Gope, M. and Gope, R., 2018. Synthetic Biology. *Omics Technologies and Bio-Engineering*, pp.63-93.
5. UK Synthetic Biology Roadmap Coordination Group (2012) *A synthetic biology roadmap for the UK*. Available at: [https://webarchive.nationalarchives.gov.uk/20130302042701/http://www.innovateuk.org/\\_assets/tsb\\_syntheticbiologyroadmap.pdf](https://webarchive.nationalarchives.gov.uk/20130302042701/http://www.innovateuk.org/_assets/tsb_syntheticbiologyroadmap.pdf)
6. Vargas-Maya NI, Bernardo F *Escherichia coli* as a Model Organism and Its Application in Biotechnology, *Escherichia coli - Recent Advances on Physiology, Pathogenesis and Biotechnological Applications*, Amidou Samie, IntechOpen, DOI: 10.5772/67306
7. Jaruszewicz-Błońska J, Lipniacki T. Genetic toggle switch controlled by bacterial growth rate. *BMC Syst Biol* [Internet]. 2017;11(1):117. Available from: <https://doi.org/10.1186/s12918-017-0483-4>
8. Lugagne J-B, Sosa Carrillo S, Kirch M, Köhler A, Batt G, Hersen P. Balancing a genetic toggle switch by real-time feedback control and periodic forcing. *Nat Commun* [Internet]. 2017;8(1):1671. Available from: <https://doi.org/10.1038/s41467-017-01498-0>
9. Huang D, Holtz WJ, Maharbiz MM. A genetic bistable switch utilizing nonlinear protein degradation. *J Biol Eng* [Internet]. 2012 Jul 9;6(1):9. Available from: <https://pubmed.ncbi.nlm.nih.gov/22776405>
10. de Jong, H. (2002). Modeling and Simulation of Genetic Regulatory Systems: A Literature Review. *Journal of Computational Biology*, 9(1), pp.67-103.
11. Atkinson, M., Savageau, M., Myers, J. and Ninfa, A. (2003). Development of Genetic Circuitry Exhibiting Toggle Switch or Oscillatory Behaviour in *Escherichia coli*. *Cell*, 113(5), pp.597-607.
12. Hillenbrand, P., Fritz, G. and Gerland, U. (2013). Biological Signal Processing with a Genetic Toggle Switch. *PLoS ONE*, 8(7), p.e68345.
13. Fiore, D., Guarino, A. and di Bernardo, M. (2019). Analysis and Control of Genetic Toggle Switches Subject to Periodic Multi-Input Stimulation. *IEEE Control Systems Letters*, 3(2), pp.278-283
14. Kobayashi, H., Kaern, M., Araki, M., Chung, K., Gardner, T., Cantor, C. and Collins, J. (2004). Programmable cells: Interfacing natural and engineered gene networks. *Proceedings of the National Academy of Sciences*, 101(22), pp.8414-8419.

15. Seong Gyeong Kim, Myung Hyun Noh, Hyun Gyu Lim, Sungho Jang, Sungyeon Jang, Mattheos A G Koffas, Gyoo Yeol Jung, Molecular parts and genetic circuits for metabolic engineering of microorganisms, *FEMS Microbiology Letters*, Volume 365, Issue 17, September 2018
16. Kis, Z., Pereira, H., Homma, T., Pedrigi, R. and Krams, R. (2015). Mammalian synthetic biology: emerging medical applications. *Journal of The Royal Society Interface*, 12(106), p.20141000./nar/gng069).
17. Weber W, et al. Conditional human VEGF-mediated vascularization in chicken embryos using a novel temperature-inducible gene regulation (TIGR) system. *Nucleic Acids Res.* 31, e69. (doi:10.1093
18. Weber W, Luzi S, Karlsson M, Sanchez-Bustamante CD, Frey U, Hierlemann A& Fussenegger M. 2009 A synthetic mammalian electro-genetic transcription circuit. *Nucleic Acids Res.* 37, e33. (doi:10.1093/nar/gkp014).
19. Balleza, E., Kim, J. and Cluzel, P. (2017). Systematic characterization of maturation time of fluorescent proteins in living cells. *Nature Methods*, 15(1), pp.47-51.
20. Voit EO, Martens HA, Omholt SW. 150 Years of the Mass Action Law. *PLOS Comput Biol* [Internet]. 2015 Jan 8;11(1):e1004012. Available from: <https://doi.org/10.1371/journal.pcbi.1004012>
21. Bartłomiejczyk A, Bodnar M. Justification of quasi-stationary approximation in models of gene expression of a self-regulating protein. *Commun Nonlinear Sci Numer Simul.* 2020;84:105166.
22. Sleight S, Bartley B, Lieviant J, Sauro H. Designing and engineering evolutionary robust genetic circuits. *Journal of Biological Engineering.* 2010;4(1):12.
23. Wieland M, Fussengger M. Engineering molecular circuits using synthetic biology in mammalian cells. *Annu Rev Chem Biomol Eng.* 2012;3:209–34.
24. S. V. Iverson, T. L. Haddock, J. Beal, and D. M. Densmore, “CIDAR MoClo: Improved MoClo Assembly Standard and New E. coli Part Library Enable Rapid Combinatorial Design for Synthetic and Traditional Biology,” *ACS Synth. Biol.*, 2016.
25. Gibson, D., Young, L., Chuang, R., Venter, J., Hutchison, C. and Smith, H., 2009. Enzymatic assembly of DNA molecules up to several hundred kilobases. *Nature Methods*, 6(5), pp.343-345
26. Foundations of Synthetic Biology Lecture Slides [Internet]. 2020 [cited 22 March 2020]. Available from: [https://bb.imperial.ac.uk/bbcswebdav/pid-1734910-dt-content-rid-5922080\\_1/courses/13728.201910/2020-Lecture8%281%29.pdf](https://bb.imperial.ac.uk/bbcswebdav/pid-1734910-dt-content-rid-5922080_1/courses/13728.201910/2020-Lecture8%281%29.pdf)
27. Cameron D, Collins J. Tunable protein degradation in bacteria. *Nat Biotechnol.* 2014;32(12):1276–1281. doi:10.1038/nbt.3053
28. Tu, Q., Yin, J., Fu, J. *et al.* Room temperature electrocompetent bacterial cells improve DNA transformation and recombineering efficiency. *Sci Rep* 6, 24648 (2016). <https://doi.org/10.1038/srep24648>
29. Salis, H.M, 2011. The ribosome binding site calculator. *Methods in enzymology*, 498, pp.19–42
30. Blazcek J, Alper HS. 2013. Promoter engineering: Recent advances in controlling transcription at the most fundamental level. *Biotechnology Journal.* 8: pp.46–58

# Appendices

## Appendix A – Project Organisation

The group was split into two main teams; the drylab and wetlab each consisting of 3 members, of whom one member of each team was responsible for adding content to the Wiki. A group member was allocated to book rooms and take meeting minutes, and another to head communications and coordination between the group and the team of supervisors.

A Gantt chart was created to plan and keep track of the group’s progress.

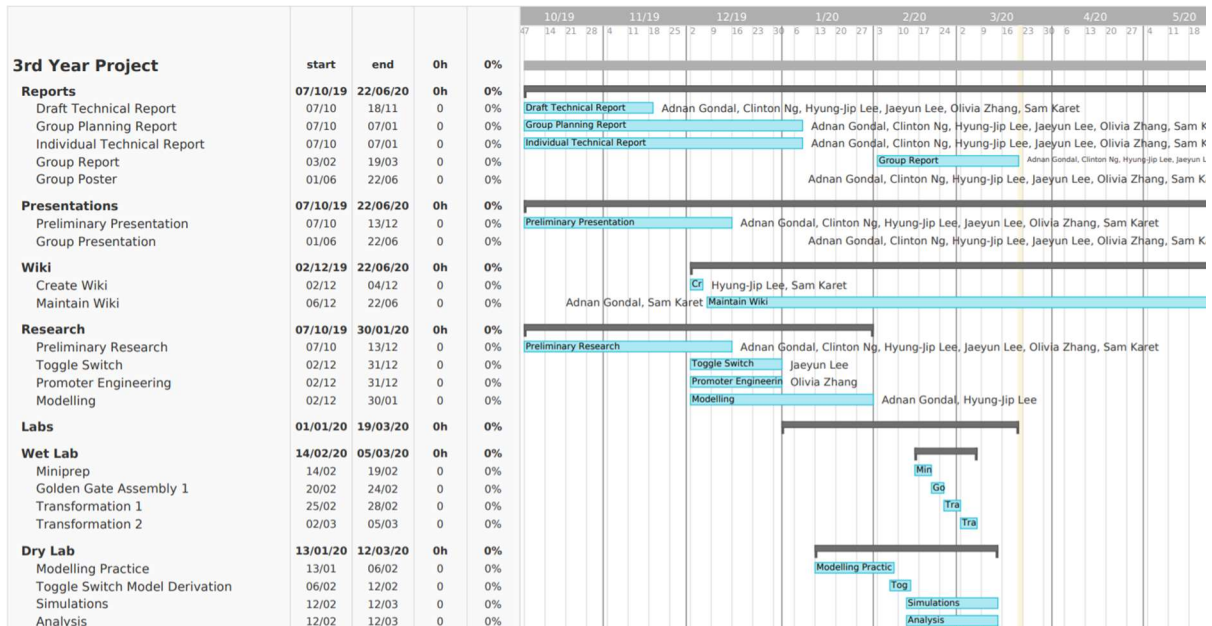


Figure 37. Gantt chart showing the project’s progress

## Appendix B – Jacobian Matrix for Toggle Switch System

The system:

$$\dot{u} = \frac{\alpha_1}{1 + v^\beta} - u$$

$$\dot{v} = \frac{\alpha_2}{1 + u^\gamma} - v$$

Jacobian Matrix:

$$J = \begin{pmatrix} \frac{\partial \dot{u}}{\partial u} & \frac{\partial \dot{u}}{\partial v} \\ \frac{\partial \dot{v}}{\partial u} & \frac{\partial \dot{v}}{\partial v} \end{pmatrix}$$

$$J = \begin{pmatrix} -1 & -\frac{\alpha_1 \beta v^{\beta-1}}{(1 + v^\beta)^2} \\ -\frac{\alpha_2 \gamma v^{\gamma-1}}{(1 + u^\gamma)^2} & -1 \end{pmatrix}$$

The eigenvalues:

$$|J - I\lambda| = 0$$

$$\begin{vmatrix} -1 - \lambda & -\frac{\alpha_1\beta v^{\beta-1}}{(1+v^\beta)^2} \\ -\frac{\alpha_2\gamma v^{\gamma-1}}{(1+u^\gamma)^2} & -1 - \lambda \end{vmatrix} = 0$$

$$(1 + \lambda)^2 = \frac{\alpha_1\beta v^{\beta-1}}{(1+v^\beta)^2} * \frac{\alpha_2\gamma v^{\gamma-1}}{(1+u^\gamma)^2}$$

$$\lambda = \pm \sqrt{\frac{\alpha_1\beta v^{\beta-1}}{(1+v^\beta)^2} \frac{\alpha_2\gamma v^{\gamma-1}}{(1+u^\gamma)^2}} - 1$$

## Appendix C – *in silico* Primer Sequences and Design Guidelines

### C1: Primer Sequences

GGG\_A:

- Forward: AGGTCCAGGCATCAAATAAA
- Reverse: TTATTAAGCTACTAAAGCGTAGTTTT

GGG\_B:

- Forward: ATGGCTTCCTCCGAGGATGT
- Reverse: TTAAGCACCGGTGGAGTGAC

### C2: Benchling parameters for automatic primer creation:

Parameter	Requirements
Min Tm for primer's binding bases	50°C
Min Tm for whole primer	60°C
Max Tm difference for primer pairs	5°C
Min length of homology/binding regions	20°C
Max length of homology/binding regions	50°C

## Appendix D – List of parts ordered from Addgene/ThermoFisher

Parts for GGO A	Parts for GGO B
DVK_AE	DVK_EF
R0040 (pTet)_AB	R0010 (pLacI)_EB
B0032m_BC	B0032m_BC
C0012m (lacI)_CD	C0040 (tetR)_CD
B0015_DE	B0015_DF
E1010m (RFP)_CD	E0040m (GFP)_CD
Positive controls:	
pJ02B2Rm_AE (constitutively expresses RFP)	
pJ02B2Gm_AE (constitutively expresses GFP)	

## Appendix E – Protocols

### Protocol E1: Pouring Agar Plates

(Taken from <https://www.addgene.org/protocols/pouring-lb-agar-plates/>)

- Equipment needed: Autoclave, Water bath, Pipetman
  - Reagents needed:
    - o 1 L Sterile H<sub>2</sub>O
    - o Sterile plates (60 mm x 15 mm)
    - o Autoclavable flask
    - o Sterile pipettes
    - o Ice bucket to hold antibiotic
    - o Ampicillin and Kanamycin
1. Measure 37g of pre-mixed LB-agar powder per L of molten agar needed
  2. Transfer the LB-agar powder into autoclavable flask.
  3. Transfer the sterile water into the bottle and swirl to form a medium/agar colloid.
  4. Cover the opening of the bottle with aluminium foil and tape the bottle with autoclave tape.
  5. Label the bottle with your initials, the date, and the bottle contents.
  6. Place the gel mix in the autoclave and run on 121 °C under 20 psi for at least 30 min.
  7. Spray down the bench with a 70% ethanol solution
  8. Label the plates with the date, medium, and antibiotic.
  9. Create a 1000xstock solution of antibiotic
  10. Retrieve your molten agar mix from the autoclave and partially submerge it in a 60 °C water bath.
  11. Light the flame at the plate pouring station and dilute antibiotic into molten gel mix using sterile technique. Swirl the bottle to ensure even distribution of the antibiotic
  12. Open one plate at a time next to the flame and begin pouring.
  13. Leave your plates out on the bench to solidify.

### **Protocol E2: Plate Streaking Protocol**

(Taken from <https://www.addgene.org/protocols/streak-plate/>)

- Equipment needed: Wire loop, Bunsen burner, Incubator, Marker
- Reagents needed: LB agar plate (with ampicillin), Bacterial stab

#### Protocol:

1. Spray workspace with 70% ethanol. Maintain sterility by working near a flame or Bunsen burner.
2. Obtain the appropriate bacterial stab or glycerol stock, and LB agar plate
3. Using a sterile loop, touch the bacteria growing within the punctured area of the stab culture or the top of the glycerol stock.
4. Gently spread the bacteria over a section of the plate
5. Using a fresh sterilized loop, drag through streak #1 and spread the bacteria over a second section of the plate, to create streak #2.
6. Using a third sterile loop, drag through streak #2 and spread the bacteria over the last section of the plate, to create streak #3.
7. Incubate plate with newly plated bacteria overnight (12-18 hours) at 37 °C.

### **Protocol E3: Miniprep Protocol: (Taken from QIAGEN Plasmid Purification Handbook)**

1. Pick a single colony from a freshly streaked selective plate and inoculate a starter culture of 2–5 ml LB medium containing the appropriate selective antibiotic. Incubate for approximately 8 h at 37°C with vigorous shaking (approx. 300 rpm).
2. Dilute the starter culture 1/500 to 1/1000 into 3 ml selective LB medium. Grow at 37°C for 12–16 h with vigorous shaking (approx. 300 rpm).
3. Harvest the bacterial cells by centrifugation at 6000 x g for 15 min at 4°C.
4. Resuspend the bacterial pellet in 0.3 ml of Buffer P1.
5. Add 0.3 ml of Buffer P2, mix thoroughly by vigorously inverting the sealed tube 4–6 times, and incubate at room temperature (15–25°C) for 5 min.
6. Add 0.3 ml of chilled Buffer P3, mix immediately and thoroughly by vigorously inverting 4–6 times, and incubate on ice for 5 min.
7. Centrifuge at maximum speed in a microcentrifuge for 10 min. Remove supernatant containing plasmid DNA promptly. Optional: Remove a 50 µl sample from the cleared lysate and save it for an analytical gel (sample 1).
8. Equilibrate a QIAGEN-tip 20 by applying 1 ml Buffer QBT, and allow the column to empty by gravity flow.
9. Apply the supernatant from step 7 to the QIAGEN-tip 20 and allow it to enter the resin by gravity flow. Optional: Remove a 50 µl sample of the flow-through and save for an analytical gel (sample 2).
10. Wash the QIAGEN-tip 20 with 2 x 2 ml Buffer QC. Optional: Remove a 220 µl sample of the combined wash fractions and save for an analytical gel (sample 3).
11. Elute DNA with 0.8 ml Buffer QF. Collect the eluate in a 1.5 ml or 2 ml microcentrifuge tubes (not supplied). Optional: Remove a 45 µl sample of the eluate and save for an analytical gel (sample 4).
12. Precipitate DNA by adding 0.7 volumes (0.56 ml per 0.8 ml of elution volume) of room-temperature isopropanol to the eluted DNA. Mix and centrifuge immediately at  $\geq 15,000$  x g rpm for 30 min in a microcentrifuge. Carefully decant the supernatant.
13. Wash DNA pellet with 1 ml of 70% ethanol and centrifuge at 15,000 x g for 10 min. Carefully decant the supernatant without disturbing the pellet.
14. Air-dry the pellet for 5–10 min, and redissolve the DNA in a suitable volume of buffer (e.g., TE buffer, pH 8.0, or 10mM Tris·Cl, pH 8.5)

**Protocol E4: Non-radioactive Phosphorylation with T4 PNK or T4 PNK (3' phosphatase minus)**

1. Set-up the following reaction in a microcentrifuge tube on ice:

1. DNA	2. up to 300 pmol of 5' termini
3. T4 PNK Reaction Buffer (10X)	4. 5 µl
5. ATP (10 mM)	6. 5 µl
7. T4 PNK	8. 1 µl (10 units)
9. Nuclease-free Water	10. up to 50 µl

2. Incubate at 37°C for 30 minutes.

3. Heat inactivate by incubating at 65°C for 20 minutes.

**Protocol E5: Annealing Oligonucleotides**

(Taken from <https://www.sigmaaldrich.com/technical-documents/protocols/biology/annealing-oligos.html>)

Equipment: Heat block or Thermocycler

Supplies: 2 mL centrifuge tubes, Pipette tips, Milli-Q® H<sub>2</sub>O, EDTA, NaCl, Trizma®, Two single-stranded oligonucleotides with complementary sequences

Protocol:

- Dissolution: Dissolve each oligonucleotide in a volume of Annealing Buffer (Concentration of each oligonucleotide needs to be 2X the desired concentration of the duplex oligonucleotide.
- Annealing: Mix Heat Block, equal volumes of the equimolar oligonucleotides in a microtube. Incubate the microtube at 95 °C for 5 min. Allow the microtube to slowly cool to room temperature (should take <60 min).
- Thermocycler: Mix equal volumes of the equimolar oligonucleotides in a PCR tube.
  - a. Use the following thermal profile
    - i. Heat to 95 °C and maintain the temperature for 2 min.
    - ii. Cool to 25 °C over 45 min
    - iii. Cool to 4 °C for temporary storage.
  - b. Centrifuge the PCR tube briefly to draw all moisture away from the lid.

**Protocol E6: Golden Gate Assembly Protocol**

- The following components were added to a 0.2 mL tube: 10–60 fmol of each DNA component, equimolar 10–50 U of BsaI , 5–50 U of T4 DNA ligase , 1× T4 DNA ligase buffer, and deionized water to at total volume of 10–60 µL.
- Reactions were performed using the following parameters: 15–40 cycles (37°C 1.5–3 min, 16 °C 3–5 min), followed by 50 °C for 5 min and 80°C for 10 min and were then held at 4 or –20°C until they were transformed.

**Protocol E7: Gibson's Assembly Protocol**

- The following components were added to a 20µl tube on ice: 0.2-1pmols of each DNA component, 10 µL Gibson Assembly Master Mix, 10µl deionised water. This was then incubated in a thermocycler at 50C for 60 minutes. Then, the samples were transferred and rested on ice to prepare for transformation.

**Protocol E8: Heat shock protocol**

1. Mix 50  $\mu$ L of 5X KCM into 200  $\mu$ L of comp cell prep, thawed on ice
2. Add 50 – 100  $\mu$ L of comp cell-KCM cocktail to DNA
3. 10min on ice (4°C)
4. 1 min 42°C
5. 1min on ice (4°C)
6. 37°C recovery for 15-60min

**Protocol E9 - PCR**

Taken from (<https://www.addgene.org/protocols/gel-electrophoresis/>)

Reagents:

- TAE: Tris-base: 242 g, Acetate (100% acetic acid) 57.1 ml, 100 ml 0.5M sodium EDTA, water
- Agarose
- Invitrogen SYBR Safe DNA Gel Stain

Pouring a Standard 1% Agarose Gel:

- Mix 1 g of agarose powder with 100 mL 1xTAE in a microwavable flask.
- Microwave for 1-3 min until the agarose is completely dissolved (
- Let agarose solution cool down to about 50 °C
- Add Invitrogen SYBR Safe DNA Gel Stain
- Pour the agarose into a gel tray with the well comb in place.

Place newly poured gel at 4 °C for 10-15 mins OR let sit at room temperature for 20-30 mins.

**Protocol E10: Gel electrophoresis**

Taken from (<https://www.addgene.org/protocols/gel-electrophoresis/>)

- Add loading buffer (HC or GF) to each of your DNA samples
- Once solidified, place the agarose gel into the gel box (electrophoresis unit).
- Fill gel box with 1xTAE (or TBE) until the gel is covered.
- Carefully load a molecular weight ladder into the first lane of the gel, and load samples into the additional wells of the gel.
- Run the gel at 80-150 V until the dye line is approximately 75-80% of the way down the gel.
- Turn OFF power, disconnect the electrodes from the power source, and then carefully remove the gel from the gel box.
- Visualize DNA fragments using UV light.

## Appendix F – Primer Sequence and Guidelines for alignment and analysis

### F1: Primer Sequence

The forward primer used was the pBRforEco primer and the reverse primer was the L4440 primer.

Name	Sequence	Location
pBRforEco (forward primer)	AATAGGCGTATCACGAGGC	In pBR322, upstream of EcoRI site, forward primer
L4440 (reverse primer)	AGCGAGTCAGTGAGCGAG	5' of MCS in L4440 vector, forward primer

**F2: Guidelines for primer design** (taken from [https://dnacore.mgh.harvard.edu/new-cgi-bin/site/pages/sequencing\\_pages/primer\\_design.jsp](https://dnacore.mgh.harvard.edu/new-cgi-bin/site/pages/sequencing_pages/primer_design.jsp))

- Primer length should be in the range of 18 and 24 bases.
- The primer should have a GC content of about 45-55%.
- The primers should have a GC-lock (or GC "clamp") on the 3' end (i.e. the last 1 or 2 nucleotides should be a G or C residue).
- The primer should have a melting temperature (T<sub>m</sub>) greater than 50°C but less than 65°C.
- The primer should not include homopolymeric runs of more than 4-5 nucleotides.
- Avoid primers with secondary structures or the potential to self-hybridize.
- Avoid designing primer upstream of homopolymeric or heteropolymeric regions (A, C, G or T repeats).
- Check primer for specificity in annealing to template (= lack of secondary priming site).
- Primer should be located at least 50-60 bases upstream of your sequence of interest.

## Appendix G – List of plate reader experiments

### G1: Control experiments (Empty Plasmids)

EXPERIMENT NAME	CELL	INDUCER ADDED
BLANK*	NONE	NONE
M9_N	NONE	NONE
M9_I	NONE	IPTG
M9_A	NONE	ARABINOSE
BL21_N	BL21	NONE
BL21_I	BL21	IPTG
BL21_A	BL21	ARABINOSE
TOP10_N	TOP10	NONE
TOP10_I	TOP10	IPTG
TOP10_A	TOP10	ARABINOSE

\*Contained no cells, plasmids or reagents.

\*\*Contained M9 media only

**G2: Control experiments (GFP and RFP – in DH5a *E. coli*)**

EXPERIMENT NAME	PLASMID	INDUCER ADDED
GFP+_N	pBW414	None
GFP+_I	pBW414	IPTG
GFP+_A	pBW414	Arabinose
RFP+_N	pECJ3D	None
RFP+_I	pECJ3D	IPTG
RFP+_A	pECJ3D	Arabinose

**G3: Test of Chassis Compatibility in  $\Delta$ lacI/ $\Delta$ araC *E. coli***

EXPERIMENT NAME	PLASMID	INDUCER ADDED
$\Delta$ LAC_PECJ3_N	pECJ3 + pZA16mflon	None
$\Delta$ LAC_PECJ3_I	pECJ3 + pZA16mflon	IPTG
$\Delta$ LAC_PECJ3_A	pECJ3 + pZA16mflon	Arabinose
$\Delta$ LAC_PECJ3B_N	pECJ3B + pZA16mflon	None
$\Delta$ LAC_PECJ3B_I	pECJ3B + pZA16mflon	IPTG
$\Delta$ LAC_PECJ3B_A	pECJ3B + pZA16mflon	Arabinose
$\Delta$ LAC_PECJ3D_N	pECJ3D + pZA16mflon	None
$\Delta$ LAC_PECJ3D_I	pECJ3D + pZA16mflon	IPTG
$\Delta$ LAC_PECJ3D_A	pECJ3D + pZA16mflon	Arabinose

**G4: Test of Chassis Compatibility in BL21 *E. coli***

EXPERIMENT NAME	PLASMID	INDUCER ADDED
BL21_PECJ3_N	pECJ3 + pZA16mflon	None
BL21_PECJ3_I	pECJ3 + pZA16mflon	IPTG
BL21_PECJ3_A	pECJ3 + pZA16mflon	Arabinose
BL21_PECJ3D_N	pECJ3D + pZA16mflon	None
BL21_PECJ3D_I	pECJ3D + pZA16mflon	IPTG
BL21_PECJ3D_A	pECJ3D + pZA16mflon	Arabinose

**Appendix H – Summary of results (all tested toggle switches)**

STRAIN	TOGGLE SWITCH CONSTRUCT	BASELINE	IPTG (0.5MM)	ARABINOSE (1MM)	DYNAMIC RANGE (FOLD)
$\Delta$ LACI $\Delta$ ARAC	pECJ3B + pZA16mflon	GFP: High RFP: Low	GFP: Low RFP: High	GFP: High RFP: Low	GFP: 7.5 RFP: 35
$\Delta$ LACI $\Delta$ ARAC	pECJ3 + pZA16mflon	GFP: High RFP: Low	GFP: Low RFP: High	GFP: High RFP: Low	GFP: 22 RFP: 175
$\Delta$ LACI $\Delta$ ARAC	pECJ3D + pZA16mflon	GFP: High RFP: Low	GFP: Low RFP: High	GFP: High RFP: Low	GFP: 10 RFP: 70
BL21	pECJ3 + pZA16mflon	GFP: High RFP: Low	GFP: Low RFP: High	GFP: High RFP: Low	GFP: 5.5 RFP: 25
BL21	pECJ3D + pZA16mflon	GFP: High RFP: Low	GFP: Low RFP: High	GFP: High RFP: Low	GFP: 10 RFP: 22.5